



DEPARTMENT OF THE AIR FORCE  
AIR FORCE RESEARCH LABORATORY  
WRIGHT-PATTERSON AIR FORCE BASE OHIO 45433

10 May 2001

MEMORANDUM FOR US EPA

NCEA (MD-52)  
RTP, NC 27711  
ATTN: ANNIE M. JARABEK

FROM: Rebecca Clewell  
AFRL/HEST  
Operational Toxicology Branch  
2856 G St, Bldg 79  
Wright-Patterson AFB, OH 45433-7400

SUBJECT: Consultative Letter, AFRL-HE-WP-CL-2001-0006, Physiologically-Based Pharmacokinetic Model for the Kinetics of Perchlorate-Induced Inhibition of Iodide in the Pregnant Rat and Fetus

1. This letter describes a physiologically-based pharmacokinetic (PBPK) model for predicting the distribution and kinetics of iodide and perchlorate. The model also predicts the perchlorate induced inhibition of thyroid iodide uptake in the pregnant rat and fetus.
2. The model is able to describe perchlorate distribution due to drinking water exposure over three orders of magnitude. It is also able to simulate the kinetic behavior of iodide in the pregnant rat and fetus at doses spanning five orders of magnitude. The model was able to predict the inhibition of iodide as a result of acute perchlorate exposure as well as the iodide kinetics reported in literature in addition to in-house data.
3. For further information, please contact me by phone: (937) 255-5150 ext. 3141, fax: (937) 255-1474 or e-mail: rebecca.clewell@wpafb.af.mil.

A handwritten signature in black ink, appearing to read "Rebecca Clewell", is positioned above the typed name.

REBECCA A. CLEWELL  
Operational Toxicology Branch

Attachments:

1. Physiologically-Based Pharmacokinetic Model for the Kinetics of Perchlorate-Induced Inhibition of Iodide in the Pregnant Rat and Fetus
2. Goodyear, C.: GD20 Inhibition Statistical Summary
3. Goodyear, C.: Serum Hormone (TSH, T<sub>3</sub>, T<sub>4</sub>) Statistical Report (Gestation Day 20)

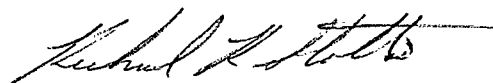
1<sup>st</sup> Ind, AFRL/HEST

10 May 2001

MEMORANDUM FOR US EPA

ATTN: MS. ANNIE JARABEK

This letter report has been coordinated at the branch level and is approved for release.



RICHARD R. STOTTS, DVM, PhD  
Branch Chief  
Operational Toxicology Branch  
Human Effectiveness Directorate

**Physiologically-Based Pharmacokinetic Model for the Kinetics of Perchlorate-Induced  
Inhibition of Iodide in the Pregnant Rat and Fetus**

Rebecca A. Clewell<sup>1</sup>, Elaine A. Merrill<sup>2</sup>, Kyung O. Yu.<sup>3</sup>,  
Deirdre A. Mahle<sup>4</sup>, Teresa R. Sterner<sup>2</sup>, Peter J. Robinson<sup>4</sup>, Jeffrey M. Gearhart<sup>4</sup>

<sup>1</sup>GEO-CENTERS, Inc.  
2856 G St, Bldg 79  
Wright-Patterson AFB, OH 45433

<sup>2</sup>Operational Technologies  
1370 N. Fairfield Rd., Ste. A  
Dayton, OH

<sup>3</sup>AFRL/HEST  
2856 G St, Bldg 79  
Wright-Patterson AFB, OH 45433

<sup>4</sup>Mantech Environmental Technology, Inc.  
PO Box 31009  
Dayton, OH 45437-009

10 May 2001

## INTRODUCTION

Ammonium perchlorate is a powerful oxidizer and the primary component of solid rocket fuel mixtures. It is also present in fireworks, ammunition and commercial fertilizers. Most perchlorate salts are highly soluble in water due to the large surface area and the small, dissociated charge of the anion. Perchlorate, the anion formed by the dissociation of the ammonium salt, has been found in the drinking water supplies of more than 11 states (Urbansky, 1998; Urbansky and Shock, 1999). Contamination of surface and groundwater by perchlorate has resulted in concern over the health effects of long-term ingestion of perchlorate (Mattie and Jarabek, 1999).

Use of perchlorate dates to the early 20<sup>th</sup> century, when its potassium salt was prescribed for the treatment of Grave's disease, an advanced form of hyperthyroidism. This treatment was eventually terminated due to complications and reported side effects (Wolff, 1998). However, perchlorate is often used in the investigation of the endocrine system's regulation of iodide. The ability of perchlorate to interfere with hormone production is a result of its ability to competitively bind to the sodium iodide symporter (NIS) in the thyroid, thereby reducing the amount of iodide available in the thyroid for hormonogenesis. NIS, a protein that resides in the basolateral membrane of thyroid epithelial cells, actively transports both  $\text{Na}^+$  and  $\text{I}^-$  ions from extracellular fluid (plasma) into the thyroid epithelial cell, simultaneously. Energy is provided by the electrochemical gradient of sodium across the cell membrane; the low intracellular concentration of sodium is maintained by sodium-potassium pumps (Ajjan *et al.*, 1998). In addition to the thyroid, active transport via NIS has been shown to occur in several tissues, including the mammary gland, salivary gland, placenta, skin, ovary and gastric juices (Brown-Grant, 1961; Spitzweg *et al.*, 1998; Kotani *et al.*, 1998). The presence of NIS and the ability of perchlorate to interfere with iodide uptake suggests a similar mode of action to the thyroid, although only the thyroid is capable of converting inorganic iodide to hormones, such as thyroxine ( $\text{T}_4$ ), triiodothyronine ( $\text{T}_3$ ) and reverse triiodothyronine ( $\text{rT}_3$ ) (Brown-Grant, 1961).

Hormone homeostasis is achieved through a complicated feedback system, wherein diminished hormone levels signal the pituitary to increase production of thyroid stimulating hormone (TSH), which in turn stimulates the thyroid to increase iodide symporter activity (Wolff, 1998). Although perchlorate has been shown to perturb the system, interfering with thyroid iodide uptake and serum hormone concentrations, the body's compensatory mechanism is able to bring the system back to equilibrium. Drinking water studies with perchlorate have demonstrated this compensation of iodide uptake and hormone levels in the male, pregnant female and lactating female rats (Yu *et al.*, 2000a). Male rat studies suggested a dose-dependent behavior, where the time required to return the system to a state of equilibrium was dependent upon the level of exposure to perchlorate (Yu *et al.*, 2000b).

The first two years of human life constitute a critical period in which the thyroid hormones play a major role in physical and mental development (Bakke *et al.*, 1976; Porterfield, 1994). A short-term iodide deficiency during this critical window has been shown to produce lifelong consequences. In humans, gestational iodide deficiency and hypothyroidism have been

associated with increased incidence of stillbirths, congenital abnormalities, lowered IQ, mental retardation and impaired hearing resulting from abnormalities in the inner ear (Delange, 2000; Hetzel, 1989 and Dobbing, 1974 as cited in Gokmen and Dagu, 1995; Porterfield, 1994; Haddow *et al.*, 1999; Klein *et al.*, 1972). In rats, studies have shown developmental hypothyroidism to result in brain cell disorganization and delayed onset of puberty and estrus (Bakke *et al.*, 1976; Clos *et al.*, 1974).

By the twelfth week of gestation in a human (Porterfield, 1994; Roti *et al.*, 1983), or gestational days 18 to 20 for the rat (Geloso, 1961 as cited in Eguchi *et al.*, 1980), the fetus has a functional thyroid-pituitary axis, is sequestering iodide and is also beginning to synthesize and secrete its own hormones (Geloso, 1961 and Nataf and Sfez, 1961 as cited in Eguchi *et al.*, 1980). Eguchi *et al.* (1980) further contend that a reciprocal relationship (or the thyroid-pituitary feedback) is in place by days 19 through 20 of gestation in the rat. The iodine needed for fetal hormone production is obtained from the mother during gestation. Iodine is thought to pass freely through the human placenta and has been shown to be actively concentrated by the placenta in the rat (Roti *et al.*, 1983; Brown-Grant, 1961).

In response to the concern about gestational perchlorate exposure, a physiologically-based pharmacokinetic (PBPK) model was developed to predict the distribution of perchlorate within the pregnant and fetal rat through gestation and at birth, and to predict the short-term effect of acute perchlorate exposure on iodide kinetics, including iodide uptake in the maternal thyroid. Mathematical equations are used to describe the uptake, excretion, placental transfer and inhibition kinetics of perchlorate and iodide within the dam and fetus. Modeling approaches to gestational growth of the dam and fetus are based on the work of O'Flaherty *et al.* (1992) with weak acids and Fisher *et al.* (1989). The purpose of this paper is to report the progress to date on this pregnancy model. Currently, perchlorate distribution data in pregnancy were only available for drinking water exposure. Acute time course data were available for radiolabeled iodide ( $^{125}\text{I}$ ), and inhibition data were available for  $^{125}\text{I}$  after exposure to  $\text{ClO}_4^-$  in both acute and drinking water scenarios. As such, acute perchlorate kinetics can only be validated, within the present version of the model, by the prediction of iodide inhibition.

## METHOD

### Supporting Experiments

**Drinking Water Study.** Perchlorate drinking water experiments used in model development were performed at AFRL/HEST. Pregnant dams of the Sprague-Dawley strain were exposed to drinking water treated with perchlorate from gestational day (GD) 2 through 20, at perchlorate doses of 0.0, 0.01, 0.1, 1.0 and 10.0 mg/kg-day. GD 0 was determined by the presence of a vaginal plug. Both dams and fetuses were sacrificed on GD 20 and maternal and fetal serum analyzed for free and total thyroxine (fT<sub>4</sub> and tT<sub>4</sub>), triiodothyronine (T<sub>3</sub>) and TSH. Maternal serum, thyroid, skin, GI contents, placenta and amniotic fluid were analyzed for perchlorate at all of the above doses. Fetal serum, skin and GI tract were also analyzed for perchlorate at all of the

doses. Two hours before sacrifice, the dams were given *iv* doses of 33 mg/kg radiolabeled  $^{125}\text{I}^-$  with carrier. Tissue concentrations of iodide were measured in order to determine the inhibition in the various tissues after long-term exposure to  $\text{ClO}_4^-$ . These studies are described in detail in another report (Yu *et al.*, 2000a).

**Preliminary Iodide Kinetics Study.** A preliminary study of  $^{125}\text{I}^-$  kinetics was performed by AFRL/HEST, in which timed-pregnant dams of the Sprague-Dawley strain were exposed via tail vein injection to a tracer dose (average dose = 2.19 ng/kg bodyweight (BW)) of the radiolabeled anion on GD 20. Dams (n=6) were sacrificed at 0.5, 2, 4 and 8 hours post-dosing. Maternal serum, thyroids, skin, GI contents, placenta and mammary gland tissue, as well as fetal serum, skin and GI tract were collected and analyzed for iodide content at each time point. Serum was pooled for all fetuses within a litter, due to limited sample volume. Fetal skin and GI tract were analyzed individually.

**Iodide Inhibition Kinetics Study.** A more in-depth study was performed by AFRL/HEST, in which Sprague-Dawley timed-pregnant dams were given 1.0 mg/kg BW  $\text{ClO}_4^-$  via tail vein injection on GD 20; control rats were given saline. The perchlorate or saline dose was followed at two hours post-dosing with a tail vein injection of carrier free  $^{125}\text{I}^-$  at an average dose of 1.87 ng/kg BW. Dams (n=6) were sacrificed after 0.5, 1, 2, 4, 8, 12 and 24 hours. Maternal serum, thyroids, skin, GI contents, placenta, mammary gland tissue, and fetal serum, skin and GI tract were collected and analyzed for iodide content at each time point. Serum was again pooled for all fetuses within a litter. Fetal skin and GI tract were analyzed individually. At this time, only the maternal serum, maternal thyroids and fetal serum from this study were available for use with the model. Further validation of the model structure will be performed at a later time with the remaining data.

### Literature Studies

**Versloot *et al.* (1997).** Versloot and coauthors measured  $^{125}\text{I}^-$  as % of dose in maternal and fetal thyroid, mammary gland, placenta and fetal carcass without the thyroid. Pregnant Wistar rats (BW =  $300 \pm 5$  g) were given an injection of 10  $\mu\text{Ci}$  carrier free  $^{125}\text{I}^-$  into the right vena jugularis on GD 19. Measurements of the maternal thyroid were taken at 4 and 24 hours post-dosing. Mammary gland, placenta, fetal thyroid and fetal carcass minus the thyroid were taken only at 24 hours post-dosing.

**Sztanyik and Turai (1988).** Sztanyik and Turai measured the uptake of iodide into the placenta and fetal whole body 24 hours post-dosing. Five groups of CFY albino rats (BW = 200 to 250 g) were dosed intraperitoneally with 370 kBq (0.081 ng) carrier free  $^{131}\text{I}^-$  on GDs 17, 18, 19, 20 and 22 of gestation. Although this is a different strain of rat, the GD 20 fetal weights (average BW = 4.088 g) compare favorably with those seen on GD 20 in the Sprague-Dawley fetus. As a result, the GD 20 time point was used in the model as means of validating GD 20 parameters for iodide

across different data sets and doses. Placental and whole body fetal  $^{131}\text{I}$  were measured in a well-type scintillation detector.

**Feldman *et al.* (1961).** Feldman and coauthors measured the uptake of iodide into the fetal thyroid and rest of body carcass on GDs 16, 17, 18 and 19 in pregnant female Holtzman rats. A single subcutaneous injection was given to the dam, containing 50  $\mu\text{Ci}$  of  $^{131}\text{I}$  on each of the days mentioned above. Fetal thyroid and carcasses were then measured at 24 hours post-dosing.

## Model Structure

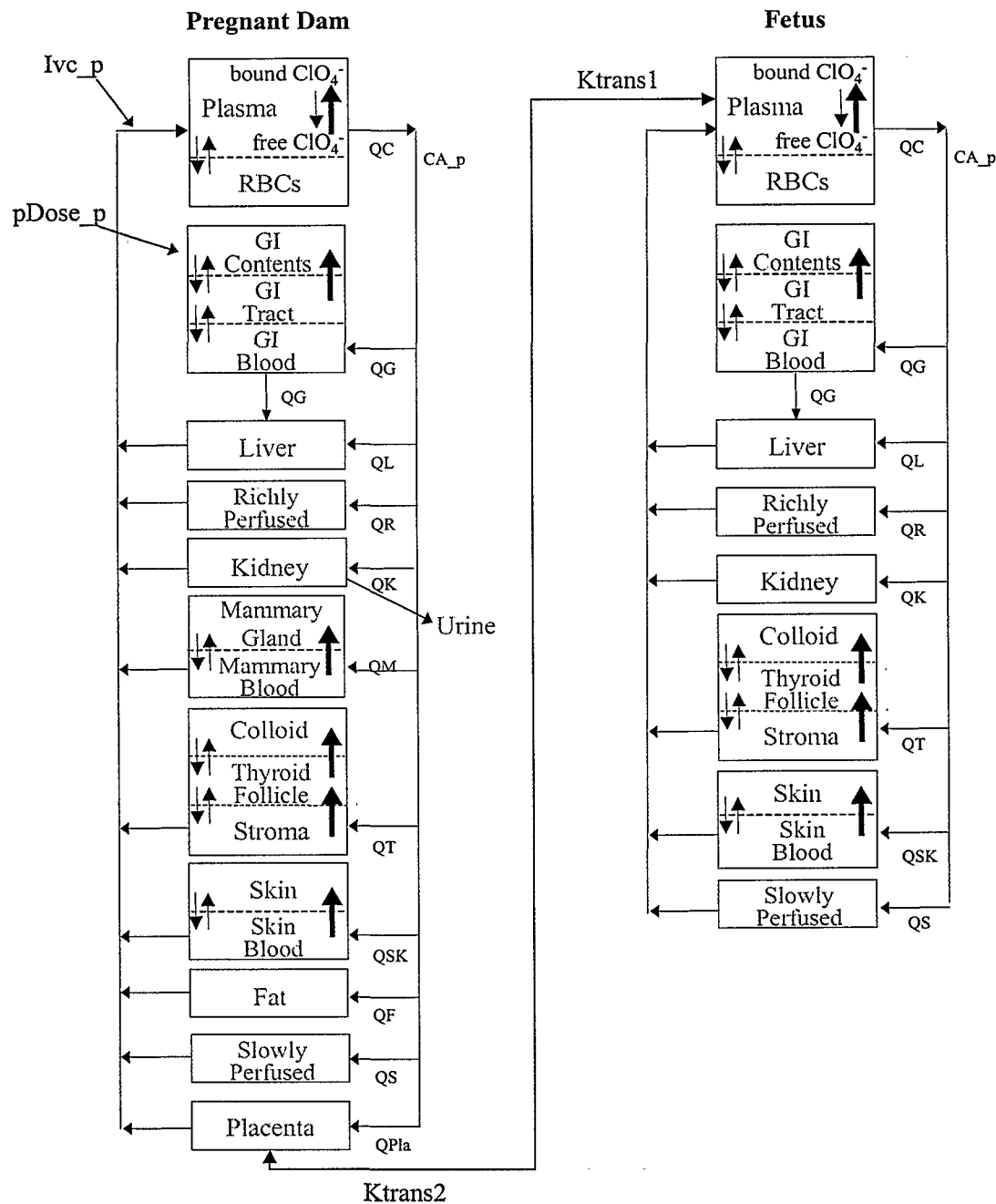


Figure 1. Schematic of PBPK models for pregnant dam (left) and fetus (right).

**Model Compartments.** The model consists of two lumped compartments (slowly and richly perfused tissues), a plasma compartment and separate compartments for the thyroid, skin, stomach, kidney, liver, fat, mammary gland and placenta. The gut and thyroid consist of three



sub-compartments representing the stroma, follicle and colloid in the case of the thyroid, and the capillary bed, tract and contents in the gut. The models also include skin and mammary gland compartments, consisting of two sub-compartments each that represent the capillary bed and tissue. The active uptake into the thyroid colloid, GI contents and skin tissue were described with Michealis-Menten terms for saturable processes (bold arrows in Figure 1). Permeability area cross products and partition coefficients were used to describe the first order movement of the anion ( $\text{ClO}_4^-$ ) between the capillary bed, tissue and inner compartments (small arrows), which results from the inherent electrochemical gradient within the tissues. The two-compartment mammary was described with both diffusion of iodide and active uptake by the symporter. The kidney, liver, fat and placenta compartments were described with partitions and blood flows. The binding of perchlorate in the blood was described with a saturable term for the association of the  $\text{ClO}_4^-$  anions to the binding sites and a first order clearance rate for the dissociation. Urinary clearance and placental-fetal transfer of the anions were represented by first order clearance rates.

Perchlorate was modeled in a similar manner to iodide, based on the shared affinity for the NIS. Tissues that have exhibited evidence of NIS and were found to significantly concentrate perchlorate and/or iodide were selected as compartments in the structure of the model. These tissues with active uptake include the thyroid, skin and gastrointestinal (GI) contents. Although several other tissues have been known to sequester iodide and perchlorate in the rat and human, such as the salivary gland, ovary, placenta and choroids plexus (Brown-Grant, 1961; Honour *et al.*, 1952; Spitzweg *et al.*, 1998; Kotani *et al.*, 1998), the amount of iodide and perchlorate in these tissues were too small to affect plasma concentrations. Therefore, these tissues were either described with effective partitioning or were lumped with the richly and slowly perfused compartments in an effort to simply the model. GI contents and thyroid tissue have been found consistently in experiments to retain higher concentrations of injected perchlorate and iodide than plasma in both the rat and human (Wolff, 1998; Halmi and Stuelke, 1959; Chow *et al.*, 1969; Yu *et al.*, 2000a and 2000b).

The behavior of perchlorate and iodide in the skin are not as well studied as the thyroid and GI contents. However, there are a few studies with measured values for either perchlorate or iodide in skin. Yu *et al.* (2000b) found  $^{36}\text{ClO}_4$  in male rat skin at higher concentrations than plasma several hours after *iv* administration, and a second paper by Yu *et al.* (2000a) reported skin to plasma ratios greater than one in lactating and pregnant dams, GD20 fetuses and PND 5 and 10 pups, after chronic dosing of perchlorate via drinking water. Zeghal *et al.* (1995) examined the effects of perchlorate on the iodine composition of rat skin. Although Zeghal did not directly measure skin perchlorate, they reported a significant reduction in skin iodide in young and adult rats after its administration, suggesting competitive inhibition.

Iodide has also been reported at higher concentrations in the skin than plasma after *iv* dosing, but the results have not been as consistent as those seen with perchlorate. Brown-Grant and Pethes (1959) observed skin:serum ratios greater than one in adult male rats and young pups. Skin:serum ratios were not as high in female rats and they did not find the same behavior in the skin of guinea pigs or mice. Yu *et al.* (2000a) reported skin: serum iodide ratios close to one in rats dosed with radiolabeled iodide intravenously. Skin was therefore described utilizing terms for active uptake in both the perchlorate and iodide models of the pregnant dam and fetus.

Although it has been suggested that the placenta may contain the capability for active uptake in the rat, intra-laboratory data do not indicate placenta:plasma levels greater than one for perchlorate or iodide (Yu *et al.*, 2000a) and unpublished iodide time course data indicate that the behavior of iodide in the placenta closely mirrors that of the plasma. Thus, the placenta was simulated with a single, flow-limited compartment. The mammary compartment has been shown to concentrate both perchlorate and iodide during lactation. However, the mammary NIS is regulated by hormones produced during lactation, and has been found to increase at the onset of lactation (Tazebay *et al.*, 2000). This concentrating mechanism does not appear to be as established during pregnancy. Studies by Yu *et al.* (2000a) report mammary gland:plasma ratios of less than one for perchlorate. However, mammary gland perchlorate levels are slowly built up and remain high well into the clearance phase of the serum. This behavior suggests a very slow diffusion between the mammary gland and blood. Consequently, the mammary gland was described with two compartments and diffusion limitation. Partitioning into the mammary, placenta and other diffusion-limited compartments is based on effective partitioning. This effective partitioning is probably very similar to the thyroid, in which an electrochemical gradient is responsible for allowing the  $\text{ClO}_4^-$  anion to move between the serum and the tissue (Chow and Woodbury, 1970).

The kidney, liver, fat and plasma were also separately defined within the general structure of the model. These tissues do not maintain  $\text{ClO}_4^-$  or iodide concentrations greater than the plasma and therefore do not contain terms for active uptake. The rapid urinary clearance of perchlorate (Yu *et al.*, 2000b) called for the inclusion of a kidney compartment in the model. A liver compartment was also utilized, due to its significant impact on iodide homeostasis. The majority of extrathyroidal deiodination takes place within the liver. Although the model does not currently include hormone production or deiodination, the future editions of the model will require the inclusion of a liver compartment. Fat was primarily added as an exclusionary compartment. The changing fat content in the pregnant animals could very likely alter the kinetics of perchlorate and iodide, since the polar anions would not be easily absorbed into fatty tissue.

High serum perchlorate concentrations at the low doses (Yu *et al.*, 2000a and 2000b) required the use of plasma binding in model simulations. The potential for perchlorate binding to protein is a subject that has not been well studied. However, the inclusion of binding is supported by the consistency between the three rat models and a few studies found in the literature, which explored the possibility of perchlorate binding to plasma proteins.

Shishiba *et al.* (1970) studied the effect of perchlorate on the free thyroxine ( $\text{fT}_4$ ) fraction in human blood. They found that perchlorate interfered with the binding of  $\text{fT}_4$  to prealbumin and albumin, but not thyroglobulin (TBG). Yamada (1967) reported an increased  $\text{fT}_4$  fraction in rat blood after administration of perchlorate. While Yamada found perchlorate to have a greater affect than thiocyanate ( $\text{SCN}^-$ ) in rats, Shishiba found perchlorate to have less affect in human blood. These studies suggest a species difference in protein/perchlorate interaction in the blood. Studies performed by Hays and Green (1973) on pertechnetate (an anion with a mechanism similar to that of perchlorate) found that perchlorate blocked the binding of pertechnetate to human serum albumin.

Carr (1952) measured perchlorate binding in bovine albumin. He found that perchlorate bound to nearly the same extent as thiocyanate ( $\text{SCN}^-$ ). Perchlorate binding in human serum was measured by Scatchard and Black (1949). Their studies also revealed that perchlorate binding was very similar to that of  $\text{SCN}^-$ . It is likely, therefore, that the mode in which perchlorate is able to prohibit albumin binding in human serum is by reversibly binding to the albumin via weak covalent interactions. This binding, although not measured directly in the rat, is evidenced through the displacement of  $\text{T}_4$  in rat serum. Given that perchlorate demonstrates a similar or slightly smaller ability to bind to albumin or prealbumin in human serum, it is feasible to assume from Shishiba's studies that perchlorate is bound to a greater extent in rat serum. This is also supported by the fact that thyroxine is primarily transported by albumin in rats as opposed to TBG in humans, which was shown not to be affected by perchlorate. Thus, it is reasonable to assume that protein binding would have a greater effect on the distribution and clearance of the anion in the rat as opposed to the human.

The structure of the fetal perchlorate model is similar to that of the pregnant rat, with the exception of the mammary gland and placenta compartments. In order to simplify the model, all of the fetuses from a single litter were combined in the structure of the model, essentially viewing the individual fetuses as one entity, or one large fetus. The dose to the fetus is based on the transfer of perchlorate from the maternal placenta to the serum of the fetus, rather than through direct exposure to the drinking water. Though a kidney is included in the fetal model, urinary excretion is not used to identify the loss of perchlorate for the fetus. Since the ability to produce urine is not well developed until after parturition, the loss from the fetus is described as first order clearance from the fetal arterial blood to the placenta.

**Growth and Changing Parameters.** The pregnancy model attempts to describe perchlorate distribution in a highly dynamic system. In addition to total body weight changes in the dam and fetus, maternal mammary tissue and blood flow, cardiac output, fractional body fat, placenta and fetus body weight and fractional body fat are also changing with respect to time. Growth equations, based on O'Flaherty *et al.* (1992) were used in ACSL (Advanced Continuous Simulation Language, Aegis Technologies Group, Inc.) to account for these changes. All tissue volume and blood flow values were adjusted with respect to the changing parameters.

**Dosing Procedures.** In order to simulate the daily dosing regimen of the drinking water experiment, the rats were assumed to drink at constant rate for 12 of the 24 hours per day (1800 to 0600 hours). A pulse function in ACSL was used to introduce drinking water to the GI contents of the dam for the first 12 hours of each 24-hour period, and then to stop dosing while the rat was presumably sleeping. Intravenous (*iv*) dosing was introduced into the venous blood compartment of the model. Intraperitoneal injection was introduced into the model in the same manner as the *iv* dosing. The fetus was constantly exposed to maternal perchlorate and iodide via the placenta.

## Model Parameters

Physiological and chemical specific parameters for iodide and perchlorate are listed with the sources from which they were obtained in Tables 1 through 3. Whenever possible, physiological and kinetic parameters were taken from literature or experimental data. Allometric scaling is employed to account for the difference in parameters due to the variations in body weight of male, female and fetal rats. The following equations illustrate the method of allometric scaling applied to the maximum velocity (Vmax), clearance values (K), tissue volumes (V) and blood flows (Q) in the dam. A value of C following the parameter name indicates the value of the parameter before allometric scaling and X represents the tissue of interest.

$$V_{\max\_X} = V_{\max c\_X} * BW^{3/4}$$

$$ClX = ClXc * BW^{3/4}$$

$$VX = VXc * BW$$

$$QX = QXc * BW^{3/4}$$

Fetal values were scaled in the same manner as the maternal parameters. However, since the model actually represents several fetuses, it was necessary to first scale the values for the individual fetus and then adjust for the total number of fetuses in the litter. The method for scaling the fetal parameters allometrically are given below, where *F* indicates that the parameter is a fetal value and *numfetus* is the number of fetuses in the litter.

$$V_{\max\_XF} = \left( V_{\max c\_XF} * BW_{\_F}^{3/4} \right) * numfetus$$

$$ClX_{\_F} = \left( ClXc_{\_F} * BW_{\_F}^{3/4} \right) * numfetus$$

$$VX_{\_F} = (VX_{\_F} * VXc * BW_{\_F}) * numfetus$$

$$QX_{\_F} = \left( QXc_{\_F} * BW_{\_F}^{3/4} \right) * numfetus$$

## Physiological Parameters

The physiological description of the maternal and fetal rat during gestation is based on O'Flaherty *et al.* (1992). However, growth descriptions, body weights and organ descriptions were optimized for use within this particular model structure. The model is able to account for differences in gestation time, pup birth weight and litter size between experiments and strains of rats. Growth equations and parameters, which change over time, were described with mathematical descriptions of available literature and experimental data.

**Maternal Tissues.** The body weight of the dam is known to change significantly throughout the relatively short gestation time in the rat (21 days). However, the traditional approach utilizing

allometric scaling to describe tissue growth in relation to the change in body weight is not a sufficient description for the changes taking place during pregnancy. As opposed to the typical growth scenario, organs and tissues cannot be assumed to increase at the same rate in this dynamic system. Rather, a few tissues, such as the placenta, fetal volume and mammary tissue, are growing at an accelerated rate in comparison to the other organs. These parameters require additional descriptions for their growth beyond the previously described allometric scaling by body weight.

Since the growth of the other tissues is negligible in comparison to the change in the placenta, mammary gland, fat and fetal volume, the total change in the maternal body weight was simply described as the change in these four volumes added to the initial (pre-pregnancy) body weight ( $BW_{init}$ ). All other maternal organs were assumed to remain constant and were scaled allometrically relative to the initial body weight. Values for parameters unchanged by pregnancy are shown in Table 1, along with the sources from which they were obtained.

Mammary tissue growth during gestation was described by Knight and Peaker (1982). Based on their work, mammary tissue growth is described as a linear process, where the mammary reaches a maximum volume for gestation on GD21 of 4.6% of the maternal body weight. The following equation was fit to data provided on the growth of mammary tissue in Hanwell and Linzell (1973) and was used in the model to describe mammary gland growth, where  $VM$  is the mammary gland volume (L),  $VM_{init}$  is the pre-pregnancy mammary volume (L) and  $Days$  represents the time in gestation, given in days.

$$VM = VM_{init} * (1.0 + (0.27 * Days))$$

The growth of maternal fat was also described as a linear process throughout gestation, based on the work of Naismith *et al.* (1982). Naismith reported a 40% increase in body fat throughout gestation. Thus, in the model a linear equation was employed to describe a 40% increase in body fat during the length of gestation, with an initial (non-pregnant) value of 7.0% body weight for Sprague-Dawley rats (Brown *et al.*, 1997). The following equation was used to calculate the increase in maternal body fat for the pregnancy model, where  $VF$  is the volume of fat in liters, and  $VF_{init}$  is the non-pregnant value for body fat in liters.

$$VF = VF_{init} * (1.0 + (0.0165 * Days))$$

Placental volume was described in the model as a sum of three stages of growth, based on the data of Buelke-Sam *et al.* (1982a), Sikov and Thomas (1970) and the mathematical description of data provided in O'Flaherty *et al.* (1992). The placenta volume is negligible during gestational days 1 through 5. Individual yolk sac placenta enter a stage of rapid growth between days 6 and 10 of gestation, which is described by the following equation:

$$VPl_{a_{GD6-10}} = VPl_{a_Y} = (NumFet * (8 * (Days - 6)))$$

where  $Vpl_{a_Y}$  is the volume of the yolk sac placenta,  $Vpl_{a_{GD6-10}}$  is the total volume of the placenta between days 6 and 10 in liters and  $NumFet$  is number of fetuses present. Placental growth during gestational days 6 through 10 is defined solely by this equation. Total placenta volume

changes during gestational days 10 through 21 (parturition) are defined by two separate processes: the exponential decline in yolk sac volume and the increase in chorioallantoic placenta. The total placental change is then described as follows:

$$VPla_Y = NumFet * (32 * \exp(-0.23 * (Days - 10)))$$

$$VPla_C = 40 * (\exp(Days - 10) - 1)$$

$$VPla_{GD10-21} = VPla_Y + VPla_C$$

where  $VPla_C$  is the volume of the chorioallantoic placenta and  $Vpla_{GD10-21}$  is total volume of the placenta between GD 10 and parturition.

O'Flaherty *et al.* (1992) also describes the growth of the uterus and liver during gestation. However, for the purpose of this model, specific description of growth in these organs was not necessary. The liver is not believed to have a major role in perchlorate kinetics and since the iodide model does not describe deiodination, the description of liver growth was deemed unnecessary. Adding a description of liver growth would only bring additional complexity to the model structure without providing a real benefit to the description of perchlorate and total iodide kinetics. The use of a uterine compartment was not included in this model, due to the lack of available perchlorate and iodide data. Without pertinent data, the compartment would be purely hypothetical and could not be validated. Therefore, the uterus was considered to be part of the lumped richly perfused tissue. The transfer of perchlorate and iodide anions was sufficiently described as a placental/fetal process.

**Maternal Blood Flows.** Temporal changes in maternal cardiac output during gestation are described in the model as the sum of the initial cardiac output, given in Brown *et al.* (1997) for a non-pregnant rat, and the change in blood flow to the placenta, mammary and fat tissues. The approach of O'Flaherty *et al.* (1992) to changing blood flows was utilized in placental, mammary and fat blood flows. In the model, the fraction of cardiac output to the mammary gland and fat tissues are described as proportional to the change in volume of the tissue. The equation for the blood flow to the mammary gland ( $QM$ ) is given as an example below. The change in blood flow to the fat would be handled in the same manner, where the initial values for blood flow to the mammary ( $QM_{Init}$ ) and fat ( $QF_{Init}$ ) are 0.2 and 7.0% of cardiac output, respectively.

$$QM = QM_{Init} * \left( \frac{VM}{VM_{Init}} \right)$$

The change in blood flow to the yolk sac placenta is approximately proportional to the change in volume of the yolk sac. However, the blood flow to the chorioallantoic placenta increases at a faster rate than the change in volume. The following equations describe the blood flow to the total placenta (L/hr) based on the stages of placental growth, where  $QPla_{GD1-6}$  is the change in blood flow from conception to GD 6,  $QPla_{GD7-10}$  is the total blood flow to the placenta from GD 7 to 9,  $QPla_{GD11-12}$  is the change in blood flow from GD 11 to 12 and  $QPla_{GD13-21}$  is the change in placental blood flow from GD13 through parturition. Dividing by 24 hours gives blood flows in liters per hour.

$$QPla_{7-9} = \frac{NumFet * 0.55 * (Days - 6)}{24}$$

$$QPla_{GD11-12} = \frac{NumFet * 2.2 * \exp(-0.23 * (Days - 10))}{24}$$

$$QPla_{GD13-21} = \frac{(NumFet * 2.2 * \exp(-0.23 * (Days - 10))) + (0.1207 * (Days - 12)) * 4.36}{24}$$

**Fetal Tissues.** A three stage description of fetal growth was also described in O'Flaherty *et al.* (1992) in order to mathematically reproduce data obtained from Beaton *et al.* (1954), Sikov and Thomas (1970), Goedbloed (1972) and Buelke-Sam *et al.* (1982a). Because data are not available for fetal volume between gestational days 1 through 11, an exponential growth curve was used as a reasonable approximation of fetal growth and was fit to the first available data for fetal volume. The growth curve begins at zero liters and increases exponentially to meet the data on GD 11; it is given by the following equation, where  $Vf_{etGD1-11}$  is the fetal volume from days 1 through 11 of gestation.

$$VF_{etGD1-10} = ((0.1206 * Days) * 4.53)$$

The second stage of growth describes a slower increase in fetal volume, beginning on GD 11, based on the aforementioned data. The following equation describes the fetal volume between days 11 and 18 of gestation ( $Vf_{etGD11-17}$ ).

$$VF_{etGD11-17} = ((1.5 * (Days - 10)) * 2.8)$$

The third stage of fetal growth is described as a linear increase between days 18 and the day of parturition. The equation is dependent on the weight of the pup at the time of birth ( $PupBW$ ). This allows the model to account for the differences in birth weight encountered when simulating different data sets. The following equation represents fetal volume between days 18 of gestation and parturition ( $Vf_{etGD18-21}$ ), where  $Vf_{etGD18}$  is the volume of the fetus on GD 18.

$$VF_{etGD18-21} = \left( VF_{etGD18} + \left( \left( \frac{PupBW - VF_{etGD18}}{4} \right) * (Days - 18) \right) \right)$$

Individual fetal organ weights were assumed to increase linearly with respect to change in fetal body weight and were therefore scaled allometrically to account for changes in tissue volumes. Values for tissue volumes were taken from literature and experimental data for the fetus when available. However, most volumes were taken from adult rat data and scaled allometrically for the fetus, due to the lack of tissue data in fetuses.

Florsheim *et al.* (1966) measured thyroid and body weight of the rat fetus and pup from GD 18 through PND 22 and reported a linear relationship between the thyroid weight and body weight throughout the time period. The value given for the thyroid of the fetus in %fetal body weight for GD 19 was used in the model. On the other hand, the physiology of the developing thyroid was found by Conde *et al.* (1991) to change significantly between birth and PND 120. Conde reports a decrease in follicle volume from 61.4% to 37.2% of the total volume of the thyroid from birth to 120 days. He also reports increase in colloid volume from 18.3% of the total thyroid volume at birth to 32.5% at 120 days. In the absence of histometric data in the fetal thyroid, the follicle, colloid and stroma volumes for the fetus were described using the thyroid fractions measured at birth. The value for thyroid stroma is calculated within the model by subtracting the colloid and follicle volumes from the total thyroid volume.

The fetal body fat content was assumed to be zero in the model. This assumption is reasonable in light of the data given in Naismith *et al.* (1982). Naismith measured values for the body fat of PND 2 and 16 rat pups, corresponding to 0.16% and 3.7% of the body weight, respectively. Given that body fat quickly increases in the neonatal period, it is not unreasonable to assume that body fat in the fetus is negligible. The volume is certainly not large enough to interfere with iodide or perchlorate kinetics. All other parameters were scaled allometrically by fetal weight from the adult male rat. The male rat physiological parameters were used rather than female parameters for a couple of reasons. First, the male rat pups have been shown to be more sensitive to perturbation of hormone homeostasis by perchlorate, and therefore are considered the sensitive endpoint (Yu *et al.*, 2000a). Additionally, sufficient evidence was not found to indicate that physiological parameters between male and female rats were present in the fetus.

**Fetal Blood Flows.** Fetal blood flow was assumed to operate independently from the mother. The transfer of the chemical was accomplished via diffusion between the placenta and fetal blood. Therefore, the fetal cardiac output and blood flow to organs (as % cardiac output) were scaled allometrically from the male rat values relative to the fetal volume.

### Chemical Specific Parameters

**Clearance Values.** For all tissues in which a clearance was described (urinary clearance, transfer between placenta and fetal serum and dissociation of perchlorate from the binding sites), a clearance value was determined. Since perchlorate is quickly excreted in urine and binding has little effect on serum levels at high doses, the simulation for the 10 mg/kg-day dose group was primarily dependent on the urinary clearance value (CIUc<sub>p</sub>). The urinary clearance value for perchlorate was therefore based on the fit of the model to the serum data at the high dose. Iodide is incorporated into many of the constituents in plasma. However, it is not bound in the same manner as perchlorate to the plasma proteins (i.e., albumin). Additionally, the iodide model is currently simplified to account for the distribution of total iodine. Therefore, the urinary clearance value was determined primarily by fitting the model simulation to the iodide serum data, as blood levels were more dependent on excretion than on the amount of iodide in other tissues.



The clearance of both iodide and perchlorate between the fetal serum and maternal placenta were based on the fit of the model simulation to the fetal and maternal blood levels and to the placenta concentration. The rate of dissociation of perchlorate from the binding sites was fit to the serum data across doses. The following equation illustrates the use of clearance values in the distribution and excretion of perchlorate, where  $RAZ_y$  is the rate of excretion of chemical  $y$  by route  $Z$ ,  $CLZ_y$  is clearance value for  $y$  by excretion route  $X$  and  $CX_y$  is the concentration of  $y$  in tissue  $X$ .

$$RAZ_y = CLZ_y * CX_y$$

**Affinity Constants and Maximum Velocities.** Kinetic values for the saturable active uptake process ( $Km_p$  and  $Vmax_p$ ) were not available for perchlorate in literature nor was it determined experimentally in our laboratory. Only the affinity of iodide for NIS was cited in the literature. Gluzman and Niepomniscze (1983) derived an average Michaelis-Menten  $Km$  of  $4.0 \times 10^6$  ng/L for iodide from thyroid slices of 5 normal individuals. The thyroid slices were incubated with several medium iodide concentrations. The experimentally determined  $Km$  values for iodide are similar across species (Gluzman and Niepomniscze, 1983) and across different tissues (Wolff, 1998). This average literature value was therefore used for iodide in tissues described with active uptake.

The apical follicular membrane (between the thyroid follicle and colloid) also exhibits a selective iodide uptake mechanism. Golstein *et al.* (1992) measured a  $Km$  value of approximately  $4.0 \times 10^9$  ng/L for the transport of iodide between the thyroid follicle and colloid in bovine thyroid. Similar to the mechanism of uptake in the basolateral membrane, this apical channel also appears to be very sensitive to perchlorate inhibition and shares a similar permeability to perchlorate and iodide.

The values for perchlorate affinity were originally assumed to be the same as those for  $Km$  of iodide, due to the similar mechanism in which the two anions are transported into the tissues. Thus, the iodide values were adjusted for the difference in mass to give an estimated value for the affinity of perchlorate. However, these values were not adequate for use in the models. Several literature sources suggest that perchlorate may have a significantly higher affinity for NIS than iodide. In his 1963 paper (Wolff and Maurey, 1963) and his 1998 review, Wolff concludes that perchlorate has a greater affinity than iodide for the NIS. This assumption was based upon his work with iodide, perchlorate and several other anions actively sequestered in the thyroid. Wolff measured the  $Km$  of a few of the anions and  $Ki$ 's (inhibition constants) for several ions, including perchlorate. He found that the relative potency of inhibition by the various anions could be described with the following series:  $TcO_4^- > ClO_4^- > ReO_4^- > SCN^- > BF_4^- > I^- > NO_3^- > Br^- > Cl^-$ . Wolff reported that the measured  $Km$  values for several of these inhibiting anions were not the same as those measured for iodide. In fact, measured values for  $Km$  and  $Ki$  for several of the inhibiting anions revealed that affinity increased with increased inhibitory potency. Halimi and Stuelke (1959) suggested that perchlorate could have an affinity as much as an order of magnitude higher than that of iodide, based upon the preferential uptake of perchlorate into the GI contents and thyroid in the rat. Their studies showed perchlorate to be ten

times as effective as iodide at depressing tissue: blood ratios in both the gastric juice and thyroid. Harden *et al.* (1968) showed the same behavior in the human salivary gland. These studies, in addition to the work of Lazarus *et al.* (1974) and Chow *et al.* (1969), support the use of a lower  $K_m$  for perchlorate uptake in the tissues with sodium iodide symporter. Therefore, the perchlorate  $K_m$  values used in the models were  $2.0 \times 10^5$  for the follicular NIS ( $K_m_{Tp}$ ) and  $1.0 \times 10^8$  ng/L for the colloidal transport ( $K_m_{DTp}$ ), approximately a factor of 10 lower than those given for iodide.

Whenever possible, chemical specific parameters were kept the same in male, female, neonatal and fetal rats and humans. However, it was necessary to change a few of the parameters, including the maximum velocities ( $V_{max}$ ). The  $K_m$  values were similar between tissues and between female and male rat and human models. However, the maximum velocity or capacity differs between tissues (Wolff and Maurey, 1961). Since values for the maximum velocities for the tissues ( $V_{maxc}$ ) for perchlorate were not given in literature, the values were estimated with the model. In order to determine  $V_{max}$  with the model, the simulation for the tissue of interest was compared to various data sets with several different perchlorate dose levels. The value for  $V_{max}$  within a given compartment was then determined by the best fit of the simulation to the data.

The following equation demonstrates the use of affinity constants and maximum velocities to describe the active sequestration of a chemical into a compartment.  $RupX_y$  is the rate of active uptake of chemical  $y$  into tissue  $X$ .  $V_{max\_Xy}$  and  $Km\_Xy$  are the maximum velocity and affinity of tissue  $X$  for chemical  $y$ , respectively.  $CZ_y$  is the concentration of chemical  $y$  in tissue  $Z$ , from which the chemical is being removed in order to sequester the ion in tissue  $X$ .

$$RupX_y = \frac{V_{max\_Xy} * CZ_y}{Km\_Xy + CZ_y}$$

### Effective Partitioning.

**Perchlorate.** The highly polar perchlorate anion is not expected to partition into tissues in the classical understanding of the process. Rather, the anion responds to the electrochemical potential present across tissue membranes. Chow and Woodbury (1970) explored the relationship of these electrochemical potentials to perchlorate concentrations in the stroma, follicle and lumen in the male rat thyroid at three different doses of  $ClO_4^-$ . Their measured difference in electrical potential between the thyroid stroma and follicle can be interpreted as an effective partition coefficient for charged moieties, such as  $ClO_4^-$  and  $I^-$ , hindering the entry of negatively charged ions into the follicle. The equal and opposite potential from the follicle to the colloid enhances passage of negatively charged species into the colloid and indicates an effective partition coefficient of greater than one.

The equivalence between electrical potential differences  $\phi_i - \phi_o$  and effective partition coefficients can be estimated in the manner of Kotyk and Janacek (1977), as follows:

$$\phi_i - \phi_o = 2.303 \frac{RT}{zF} \log \frac{c_o}{c_i}$$

where  $R$  is the gas constant,  $T$  is the absolute temperature and  $F$  is the Faraday constant. At  $37^\circ\text{C}$ ,  $2.303RT/F = 61.6 \text{ mV}$ , so for a singly charged ion ( $z=1$ ), this becomes:

$$\phi_i - \phi_o = 61.6 \log \frac{c_o}{c_i} \text{ (mV)}$$

In general, the ratio of the concentrations of a species between two media is given by the partition coefficient ( $K_p$ ), where  $K_p = c_o/c_i$ . Thus, the previous equation becomes:

$$\phi_i - \phi_o = 61.6 \log K_p$$

or

$$K_p = 10^{(\phi_i - \phi_o)/61.6}$$

From Chow and Woodbury (1970), the potential difference for the stroma:follicle interface ranges from  $-58$  to  $-51 \text{ mV}$ , so from the above equation,  $K_p$  for a monovalent negatively charged ion is between  $0.114$  and  $0.149$ . Similarly, for the follicle:lumen interface,  $\phi_i - \phi_o$  ranges from  $+50$  to  $+58 \text{ mV}$ , rendering the effective  $K_p$  between  $6.48$  and  $8.74$ .

Though the electrochemical potentials were not measured in the other tissues, tissue:plasma ratios of doses large enough to saturate the active transport process were used as “effective partitions”. Effective partition coefficients for  $\text{ClO}_4^-$  in the placenta, skin, GI tract and contents were calculated from the tissue:plasma ratios measured in the  $10.0 \text{ mg/kg-day}$  drinking water dose of the gestation drinking water study (Yu *et al.*, 2000a). The  $10.0 \text{ mg/kg-day}$  dose is sufficient to cause saturation of the tissues with NIS and is therefore considered a reasonable dose for estimating the effective partition coefficients. In the drinking water studies, measurements were taken after 18 days of dosing, allowing the assumption that the system was at steady state. The  $\text{ClO}_4^-$  tissue:plasma ratios measured in the drinking water studies at the  $10 \text{ mg/kg-day}$  dose group were thus considered to be a realistic estimate of the effective partitioning within these tissues. Effective  $\text{ClO}_4^-$  partition coefficients for the skin, gastric tract and GI contents were calculated to be  $1.15$ ,  $1.8$  and  $2.3$  in the dam and fetus, respectively. The gastric tract and contents could not be separated in the fetus. Consequently, the fetal GI tract and contents were measured simultaneously. Thus, the maternal values for partitions were used for the total fetal gut. The partition coefficient for the placenta was calculated to be  $0.56$  from the  $10 \text{ mg/kg-day}$  drinking water data.

The tissues that did not contain NIS were not analyzed for perchlorate in the gestation drinking water studies performed by Yu *et al.* (2000a). Therefore, effective partition coefficients were calculated from data available in literature and from *iv* dosing studies in the male rat (Yu *et al.*, 2000b). The effective partitions for the slowly perfused (muscle), richly perfused (liver), liver, kidney and red blood cells were calculated from the tissue:plasma ratios obtained during the

clearance stage of perchlorate, after *iv* dosing with 3.3 mg/kg  $\text{ClO}_4^-$ . A dose of 3.3 mg/kg  $\text{ClO}_4^-$  is sufficient to saturate the symporter and is therefore a realistic dose for calculating effective partition coefficients.

Pena *et al.* (1976) measured tissue:blood ratios in the laying hen after intra-muscular dosing with either a single injection of 10  $\mu\text{Ci}$  or 3 sequential doses of 10  $\mu\text{Ci}$  radiolabeled  $^{36}\text{ClO}_4^-$ . Although the hen is a very different species, several of other tissues were reported to have values comparable to those found by Yu *et al.* (2000a and 2000b) in the male and female rat (0.3 vs. 0.31 in muscle, 0.1 vs. 0.1 in brain, 0.8 vs. 0.99 in the kidney). Therefore, the value of 0.05 reported for the partitioning of perchlorate into the fat of the hen was used to represent the fat in the pregnant rat and fetus. The use of this value is supported by the fact that the polarity of the perchlorate anion would severely limit the movement of  $\text{ClO}_4^-$  into fatty lipophilic tissue. Anbar *et al.* (1959) measured the mammary gland:blood ratios in the rat four hours after an intra-peritoneal injection of radiolabeled  $^{36}\text{ClO}_4^-$  (100 mg  $\text{KClO}_4$ ). They reported an effective partition of 0.66 for the rat mammary gland.

*Iodide.* Thyroid effective partition coefficients were assigned within the range calculated for perchlorate. These values are reasonable for use with the uptake of iodide, due to the electrochemical gradient, based on the fact that iodide and perchlorate have the same ionic charge and very similar ionic radii. A partition coefficient for the movement of iodide fat was not available in literature. Therefore, the values found for perchlorate were utilized in the description of the movement of iodide between fatty tissue and serum. Like perchlorate, the polarity of the iodide anion is expected to severely limit the movement of  $\text{ClO}_4^-$  into fatty, lipophilic tissue. Since the partition for iodide into the mammary was not available in literature and active uptake was apparently controlling the behavior of the time points available from experiments, the mammary gland was assigned the same partition coefficient as that given for  $\text{ClO}_4^-$  in Anbar *et al.* (1959).

Tissue:blood ratios for iodide in the liver (0.40) and muscle (0.21) given in Halimi *et al.* (1956) were used to estimate the richly and slowly perfused partition coefficients. Halimi measured organ to serum concentration ratios in rats at 1, 4 and 24 hours after administering a tracer dose of radiolabeled iodide by intravenous injection. Similar values were given in Perlman *et al.* (1941) for rabbits, five hours after subcutaneous dosing with a tracer dose of iodide. Perlman also reported a tissue:blood ratio of approximately 0.7 in the skin after *iv* dosing, which remained relatively constant out to 96 hours. Maternal and fetal skin were described using this value as a partition coefficient.

When available, iodide partition coefficients were calculated from the tissue:blood ratios measured during the clearance phase of iodide data in the tissue of interest. The preliminary iodide kinetics study described in the supporting experiments was utilized for the determination of the placenta partition coefficients. For example, GI tract and contents were determined from the clearance portion of the iodide kinetic study in the adult male rat, performed by Yu *et al.* (2000b).

Permeability area cross products (PA) are used to limit the movement of the anion between tissues where multiple compartments were described with partition coefficients. Reducing the value of a PA slows the movement between the compartments; increasing the PA allows the anion to move between compartments more quickly. These values were fit to available data by comparing the model simulation to data. Effective partitioning into a tissue can be seen in the following equations, utilizing both PA's and partition coefficients, where  $RAXB\_y$  is the rate of change of chemical  $y$  in the blood of compartment  $X$  and  $RAX\_y$  is the rate of change of chemical  $y$  in the tissue of compartment  $X$ ,  $QX$  is the fractional blood flow to the compartment's capillary bed,  $CA\_y$  is the arterial concentration of  $y$  and  $CVXB\_y$  is the concentration of  $y$  in the tissue blood.

$$RAXB\_y = QX * (CA\_y - CVXB\_y) + PAX\_y * \left( \frac{CX\_y}{PX\_y} - CVXB\_y \right)$$

$$RAX\_y = PAX\_y * \left( CVXB\_y - \frac{CX\_y}{PX\_y} \right)$$

**Model Equations.** The following equations represent the distribution of iodide within the thyroid, in the absence of competitive inhibition. Perchlorate and other tissues of active uptake are described in a similar manner.

$$RATB\_i = QT * (CA\_p - CVTB\_i) + PAT\_i * \left( \frac{CT\_i}{PT\_i} - CVTB\_i \right) - RupT\_i$$

$$RAT\_i = RupT\_i + PAT\_i * \left( CVTB\_i - \frac{CT\_i}{PT\_i} \right) - RupDT\_i + PADT\_i * \left( \frac{CDT\_i}{PDT\_i} - CT\_i \right)$$

$$RADT\_i = RupDT\_i + PADT\_i * \left( CT\_i - \frac{CDT\_i}{PDT\_i} \right)$$

$$RupT\_i = \frac{Vmax\_Ti * CVTB\_i}{Km\_Ti + CVTB\_i}$$

$$RupDT\_i = \frac{Vmax\_DTi * CT\_i}{Km\_DTi + CT\_i}$$

$RATB\_i$ ,  $RAT\_i$  and  $RADT\_i$  are the rates of change in perchlorate amount in the thyroid stroma, follicle and colloid, respectively.  $PAT\_i$ ,  $PADT\_i$  and  $PT\_i$ ,  $PDT\_i$  are the PA's and effective partition coefficients for the stroma:follicle and follicle:colloid membranes, respectively.  $RupT\_i$ , and  $RupDT\_i$  are the rates of active uptake of perchlorate into the follicle and colloid.  $Vmax\_Ti$ ,  $Vmax\_DTi$  and  $Km\_Ti$ ,  $Km\_DTi$  are the maximum velocities and affinity constants for the transport of perchlorate into the follicle and colloid, respectively.  $QT$  represents the fractional blood flow to the thyroid capillary bed.  $CA\_i$ ,  $CVTB\_i$ ,  $CT\_i$  and  $CDT\_i$  are the perchlorate concentrations in the arterial plasma, thyroid stroma, follicle and colloid, respectively.

The inhibited thyroid is described in the same manner as shown above, with changing only the Michealis-Menten terms for active sequestration. The following equations describe competitive inhibition of iodide uptake by perchlorate. As before,  $R_{upDT\_i}$  and  $R_{upT\_i}$  represent the rates of active uptake of iodide into the thyroid colloid and follicle, respectively. These rates are modified by the affinity of transport mechanisms in the follicle and colloid for perchlorate ( $K_{m\_Tp}$  and  $K_{m\_DTp}$ , respectively) and the concentration of  $ClO_4^-$  in the follicle and colloid ( $CT\_p$  and  $CDT\_p$ , respectively).

$$R_{upT\_i} = \frac{V_{max\_Ti} * CVTB\_i}{K_{m\_Ti} * \left(1 + \frac{CVTB\_p}{K_{m\_Tp}}\right) + CVTB\_i}$$

$$R_{upDT\_i} = \frac{V_{max\_DTi} * CT\_i}{K_{m\_DTi} * \left(1 + \frac{CT\_p}{K_{m\_DTp}}\right) + CT\_i}$$

TABLE 1: PHYSIOLOGICAL PARAMETERS

Physiological Parameters	Pregnancy		Source
Tissue Volumes (%BW)	Dam	Fetus	
Body Weight <i>BW</i> and <i>Vlfet</i> (kg)	0.280 - 0.361	0.0 - .0045	O'Flaherty <i>et al.</i> , 1992
Slowly Perfused <i>VSc</i> (%BW)	74.6	74.6	Brown <i>et al.</i> , 1997
Richly Perfused <i>VRc</i> (%BW)	11	11	Brown <i>et al.</i> , 1997
Fat <i>VFc</i> (%BW)	10.0 - 11.0	0.0	Naismith <i>et al.</i> , 1982
Kidney <i>VKc</i> (%BW)	1.7	1.7	Brown <i>et al.</i> , 1997
Liver <i>VLc</i> (%BW)	3.4	3.4	Brown <i>et al.</i> , 1997
GI Tract <i>VGc</i> (%BW)	3.60	3.60	Brown <i>et al.</i> , 1997
GI Contents <i>VGJc</i> (%BW)	7.20	7.20	Yu <i>et al.</i> , 2000a
GI Blood <i>VGBc</i> (%VG)	2.9	2.9	Altman and Dittmer, 1971
Skin Tissue <i>VSkc</i> (%BW)	19.0	19.0	Brown <i>et al.</i> , 1997
Skin Blood <i>VSkBc</i> (%VSk)	2.0	2.0	Brown <i>et al.</i> , 1997
Thyroid Total <i>VTotc</i> (%BW)	0.0105	0.0234	Malendowicz and Bednarek, 1986; Florsheim <i>et al.</i> , 1966
Thyroid Follicle <i>VTc</i> (%BW)	45.9	61.4	Malendowicz and Bednarek, 1986; Conde <i>et al.</i> , 1991
Thyroid Colloid <i>VDTc</i> (%BW)	45	18.3	Malendowicz and Bednarek, 1986; Conde <i>et al.</i> , 1991
Thyroid Blood <i>VTBc</i> (%VT)	9.1	20.3	Malendowicz and Bednarek, 1986; Conde <i>et al.</i> , 1991
Plasma <i>VPlasc</i> (%BW)	4.7	4.7	Brown <i>et al.</i> , 1997; Altman and Dittmer, 1971
Red Blood Cells <i>VRBCc</i> (%BW)	2.74	2.74	Brown <i>et al.</i> , 1997; Altman and Dittmer, 1971
Placenta <i>VPlac</i> (%BW)	0.0 -2.57	---	O'Flaherty <i>et al.</i> , 1992
Mammary Tissue <i>VMc</i> (%BW)	1.0 - 5.5	---	Knight <i>et al.</i> , 1984; O'Flaherty <i>et al.</i> , 1992
<b>Blood Flows (%QC)</b>			
Cardiac Output <i>QCc</i> (L/hr/kg)	14	14.0	Buelke-Sam, 1982a & b; O'Flaherty <i>et al.</i> , 1992
Slowly Perfused <i>QSc</i> (%QC)	24.0	24.0	Brown <i>et al.</i> , 1997
Richly Perfused <i>QRc</i> (%QC)	76.0	76.0	Brown <i>et al.</i> , 1997
Fat <i>QFc</i> (%QC)	7 - 8.1	0.0	Brown <i>et al.</i> , 1997
Kidney <i>QKc</i> (%QC)	14.0	14.0	Brown <i>et al.</i> , 1997
Liver <i>QLc</i> (%QC)	18.0	18.0	Brown <i>et al.</i> , 1997
Stomach <i>QGc</i> (%QC)	13.60	13.60	Brown <i>et al.</i> , 1997
Thyroid <i>QTc</i> (%QC)	1.6	1.6	Brown <i>et al.</i> , 1997
Mammary <i>QMc</i> (%QC)	0.2 - 1.2	---	Hanwell and Linzell, 1973
Placenta <i>QPlc</i> (%QC)	0.0 - 12.3	---	O'Flaherty <i>et al.</i> , 1992

**TABLE 2: PERCHLORATE SPECIFIC PARAMETERS**

Pregnancy Parameters	Perchlorate Values		Source
Partition Coefficients (unitless)	Dam	Fetus	
Slowly Perfused / Plasma PS	0.31	0.31	Yu <i>et al.</i> , 2000b
Rapidly Perfused / Plasma PR	0.56	0.56	Yu <i>et al.</i> , 2000b
Fat/ Plasma PF	0.05	---	Pena <i>et al.</i> , 1976
Kidney/ Plasma PK	0.99	0.99	Yu <i>et al.</i> , 2000b
Liver/Plasma PL	0.56	0.56	Yu <i>et al.</i> , 2000b
Gastric Tissue/Gastric Blood PG	0.50	1.80	Yu <i>et al.</i> , 2000a
GI Contents/GI Tissue PGJ	1.30	2.30	Yu <i>et al.</i> , 2000a
Skin Tissue/Skin Blood PSk	1.15	1.15	Yu <i>et al.</i> , 2000a
Thyroid Tissue/Thyroid Blood PT	0.13 / 2.25	0.13 / 2.25	Chow and Woodbury, 1970
Thyroid Lumen/Thyroid Tissue PDT	7.00	7.00	Chow and Woodbury, 1970
Red Blood Cells/Plasma	0.73	0.73	Yu <i>et al.</i> , 2000b
Placenta/ plasma PPL	0.56	---	Assume same as richly perfused
Mammary/Plasma PMam_p	0.66	---	Anbar <i>et al.</i> , 1959
<b>Max Capacity, Vmaxc (ng/hr/kg)</b>			
Thyroid Follicle Vmaxc_T	1.80E+03	1.80E+03	fitted*
Thyroid Colloid Vmaxc_DT	1.00E+04	1.00E+04	fitted*
Skin Vmaxc_S	6.00E+05	4.00E+05	fitted
Gut Vmaxc_G	8.00E+05	8.00E+05	fitted
Mammary Gland Vmaxc_M	3.90E+04	---	Molar equivalent to Vmaxc_Mi
Plasma Binding Vmaxc_Bp	5.00E+03	1.50E+03	fitted
<b>Affinity Constants, Km (mg/L)</b>			
Thyroid Follicle Km_T	1.00E+05	1.00E+05	Wolff, 1998
Thyroid Colloid Km_DT	1.00E+08	1.00E+08	Golstein <i>et al.</i> , 1992; Wolff, 1998
Skin Km_S	1.00E+05	1.00E+05	Wolff, 1998
Gut Km_G	1.00E+05	1.00E+05	Wolff, 1998
Mammary Gland	1.00E+5	---	Wolff, 1998
Plasma Binding Km_Bp	1.00E+05	1.00E+05	fitted
<b>Permeability Area Cross Products, (L/hr-kg)</b>			
GI Blood to GI Tissue PAGc	1.00	1.00	fitted
GI Tissue to GI Contents PAGJc	1.00	1.00	fitted
Thyroid Blood to Thyroid Tissue PATc	9.0E-5 / 6.0E-4	9.0E-5 / 6.0E-4	fitted
Thyroid Tissue to Thyroid Lumen PADTc	0.01	0.01	fitted
Skin Blood to Skin Tissue PASKc	1.00	1.00	fitted
Plasma to Red Blood Cells PRBCc	1.00	1.00	fitted
<b>Clearance Values, (L/hr-kg)</b>			
Urinary excretion CLUc	0.07	---	Yu <i>et al.</i> , 2000b
Transfer from Placenta to Fetus Cltrans1c	0.10		Yu <i>et al.</i> , 2000a
Transfer from Fetus to Placenta Cltrans2c	0.19		Yu <i>et al.</i> , 2000a
Dissociation from Plasma Binding Sites Clunbc_p	0.034	0.010	Yu <i>et al.</i> , 2000a

\* Fetus was given maternal values for Vmax (scaled by fetal body weight) in the absence of data.



**TABLE 3: IODIDE SPECIFIC PARAMETERS**

Pregnancy Parameters	Iodide Values		Iodide Source
Partition Coefficients (unitless)	Dam	Fetus	
Slowly Perfused/Plasma PS	0.21	0.21	Halmi <i>et al.</i> , 1956
Rapidly Perfused/Plasma PR	0.40	0.40	Halmi <i>et al.</i> , 1956
Fat/Plasma PF	0.05	---	Pena <i>et al.</i> , 1976
Kidney/Plasma PK	1.09	1.09	Yu <i>et al.</i> , 2000b
Liver/Plasma PL	0.44	0.44	Yu <i>et al.</i> , 2000b
GI Tissue/GI Blood PG	0.50	0.50	Yu <i>et al.</i> , 2000b
GI Contents/GI Tissue PGJ	3.50	3.50	Yu <i>et al.</i> , 2000b
Skin Tissue/Skin Blood PSK	0.70	0.70	Perlman <i>et al.</i> , 1941
Thyroid Tissue/Thyroid Blood PT	0.15	0.15	Chow and Woodbury, 1970
Thyroid Lumen/Thyroid Tissue PDT	7.00	7.00	Chow and Woodbury, 1970
Red Blood Cells/Plasma	1.00	1.00	Yu <i>et al.</i> , 2000b
Placenta/Plasma PPL	0.99	---	Unpublished GD20
Mammary/Plasma PMam <sub>p</sub>	0.66	---	Anbar <i>et al.</i> , 1959 (for ClO <sub>4</sub> <sup>-</sup> )
<b>Max Capacity, Vmaxc (ng/hr/kg)</b>			
Thyroid Follicle Vmaxc <sub>T</sub>	4.00E+04	8.00E+04	fitted
Thyroid Colloid Vmaxc <sub>DT</sub>	6.00E+07	6.00E+07	fitted
Skin Vmaxc <sub>S</sub>	6.00E+04	3.00E+05	fitted
Gut Vmaxc <sub>G</sub>	1.00E+06	2.00E+05	fitted
Mammary Gland Vmaxc <sub>M</sub>	5.00E+04	---	fitted
<b>Affinity Constants, Km (mg/L)</b>			
Thyroid Follicle Km <sub>T</sub>	4.00E+06	4.00E+06	Gluzman and Niepomnischcze, 1983
Thyroid Colloid Km <sub>DT</sub>	1.00E+09	1.00E+09	Golstein <i>et al.</i> , 1992
Skin Km <sub>S</sub>	4.00E+06	4.00E+06	Gluzman and Niepomnischcze, 1983
Gut Km <sub>G</sub>	4.00E+06	4.00E+06	Gluzman and Niepomnischcze, 1983
Mammary Gland Km <sub>M</sub>	4.00E+06	---	Gluzman and Niepomnischcze, 1983
<b>Permeability Area Cross Products, (L/hr-kg)</b>			
GI Blood to GI Tissue PAGc	0.80	0.80	fitted
GI Tissue to GI Contents PAGJc	0.60	0.60	fitted
Thyroid Blood to Thyroid Tissue PATc	1.000E-04	1.000E-04	fitted
Thyroid Tissue to Thyroid Lumen PADTc	1.00E-04	1.00E-04	fitted
Skin Blood to Skin Tissue PASKc	0.10	0.02	fitted
Plasma to Red Blood Cells PRBCc	1.00	1.00	fitted
<b>Clearance Values, (L/hr-kg)</b>			
Urinary excretion CLUc	0.03	---	Unpublished GD 20 Iodide <i>iv</i> Data
Transfer from Placenta to Fetus Cltrans1c	0.06		Unpublished GD 20 Iodide <i>iv</i> Data
Transfer from Fetus to Placenta Cltrans2c	0.12		Unpublished GD 20 Iodide <i>iv</i> Data

## RESULTS AND DISCUSSION

### Model Development

**Perchlorate Parameterization.** In order to describe the blood perchlorate concentrations at the lower doses (0.01 and 0.1 mg/kg-day), it was necessary to account for the serum binding of perchlorate. Figures 2 through 5 illustrate the importance of binding in the model simulations of both maternal and fetal serum. Binding does not have a noticeable effect on the plasma concentrations in the highest dose. However, as the perchlorate dose decreases, the effect of binding is more pronounced. Therefore, at lower levels, a larger percent of the injected dose will be bound. As the amount consumed is increased, the binding process is saturated and eventually the amount of perchlorate that is bound is negligible in contrast to the large amount of free perchlorate in the plasma. This is to be expected, since the number of binding sites is limited. In these and subsequent plots, the solid lines indicate the model prediction and cross bars indicate the mean  $\pm$  the standard deviation (SD).

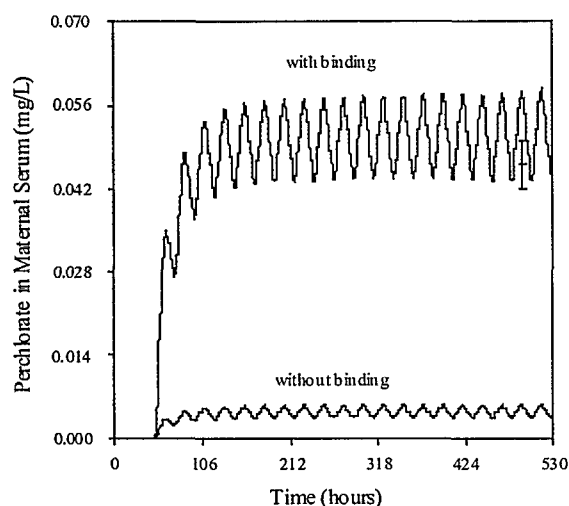


**Figure 2.** Maternal plasma perchlorate concentration at the 0.01 mg/kg-day dose, predicted with and without plasma binding

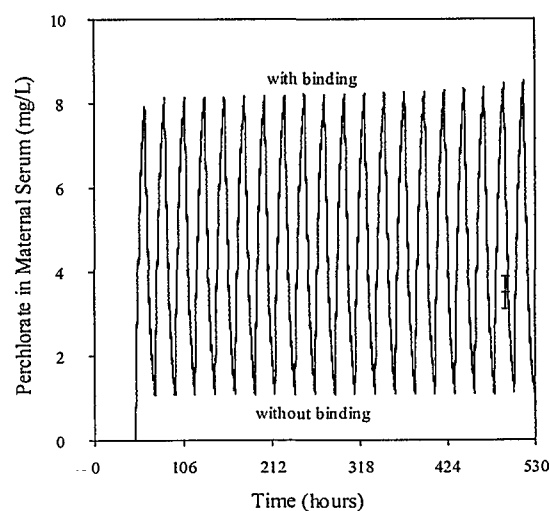


**Figure 3.** Maternal plasma perchlorate concentration at the 10.0 mg/kg-day dose, predicted with and without plasma binding

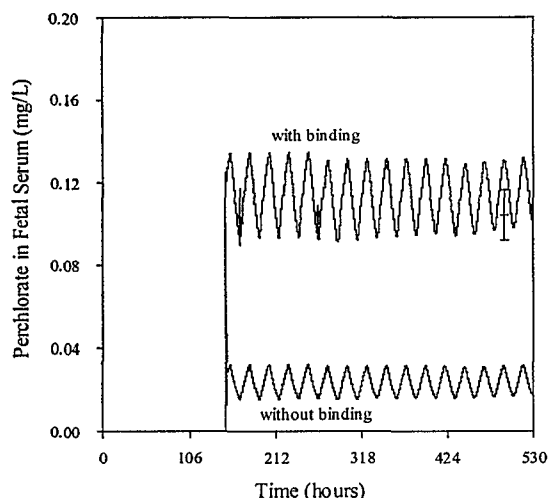


**Figure 4. Fetal plasma perchlorate concentration at the 0.1 mg/kg-day dose, predicted with and without plasma binding**

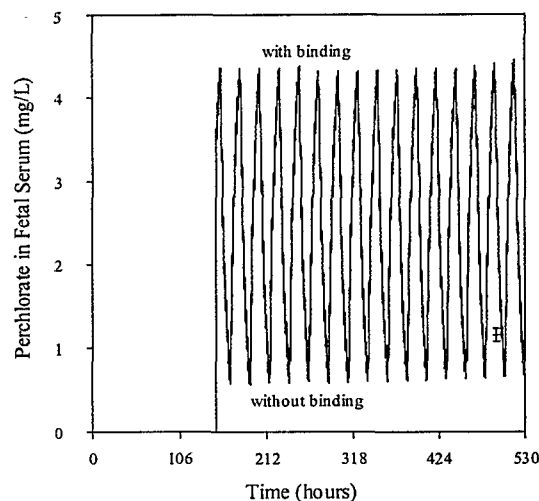


**Figure 5. Fetal plasma perchlorate concentration at the 10.0 mg/kg-day dose, predicted with and without plasma binding**

Perchlorate model parameterization was performed using the data obtained from the GD 20 drinking water studies. Optimized kinetic parameters ( $V_{max}$  and  $PA$ ) were determined by fitting the model simulation to the experimental data. Other parameters, such as partition coefficients were obtained from literature or experiment as described previously. Figures 6-9 show the serum, thyroid, skin, and GI content perchlorate concentrations at GD 20 in the pregnant dam at the 0.01, 0.1, 1.0, and 10.0 mg/kg-day doses.

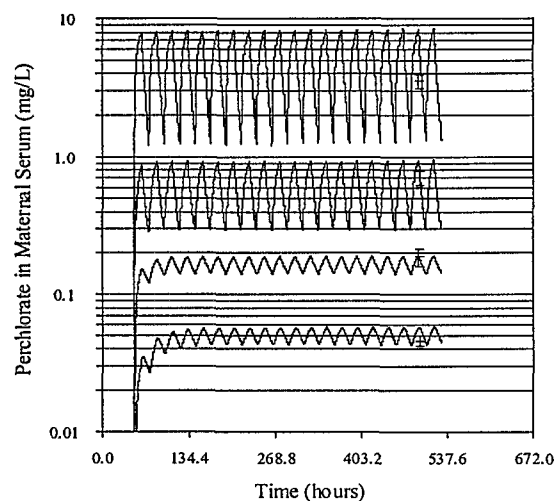


**Figure 6. Perchlorate concentration in the serum of the dam at the 0.01, 0.1, 1.0 and 10.0 mg/kg-day dose groups on GD 20**

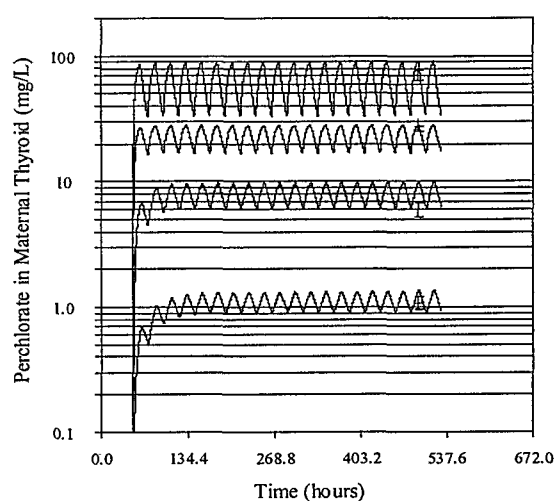


**Figure 7. Perchlorate concentration in the thyroid of the dam at the 0.01, 0.1, 1.0 and 10.0 mg/kg-day dose groups on GD 20**

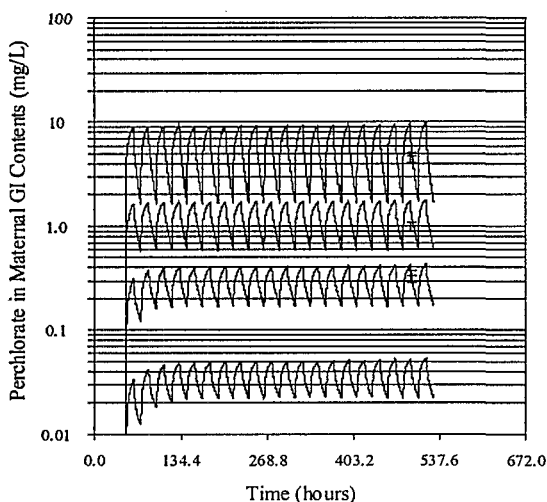


**Figure 8. Perchlorate concentration in the GI contents of the dam at the 0.01, 0.1, 1.0 and 10.0 mg/kg-day dose groups on GD20. Data in 0.01 mg/kg-day dose were below analytical detection.**

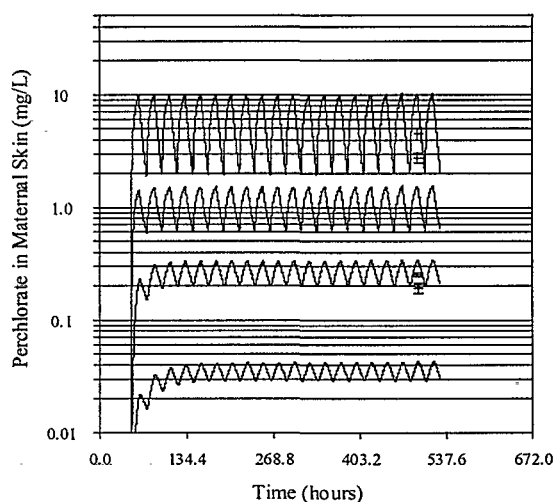


**Figure 9. Perchlorate concentration in the skin of the dam at the 0.01, 0.1, 1.0 and 10.0 mg/kg-day dose groups on GD 20. Data from 0.01 and 1.0 overlap with the 0.1 and 10.0 mg/kg-day dose data, respectively.**

Since saturation of the symporter occurs between the 1.0 and 10.0 mg/kg-day dose groups, the influence of  $V_{max}$  in the tissues was primarily in the 0.01 to 1.0 mg/kg-day doses. Thus, the fit of the model simulation to the data in the lower three doses was used to determine the values for  $V_{max}$  in the tissues. On the other hand, the  $V_{max}$  did not have a significant effect on the highest dose. The model fits to the 10 mg/kg-day dose group were primarily affected by the partition coefficients and PA values. The PA values in the tissues were obtained by fitting the highest dose to the 10 mg/kg-day data in the tissues. Maternal placenta, mammary gland and GI tract concentrations were available at the 10 mg/kg dose only. These tissues were used to verify the applicability of the assigned partition coefficients to the model. Since mammary gland was not available for the 0.01 through 1.0 mg/kg-day dose groups, it was not possible to fit the  $V_{max}$  value to data at which the symporter has a significant effect. Therefore, the  $V_{max}$  in the mammary gland was given assigned of the molar equivalent of the iodide  $V_{max}$ . This is probably a reasonable value in the non-lactating gland. Figures 10 through 12 demonstrate the fit of the model to the GI tract, mammary and placenta in the pregnant dam.

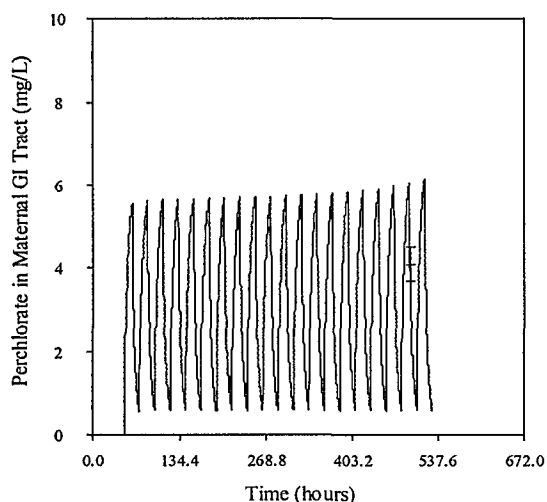


**Figure 10. Perchlorate concentration in the maternal GI tract at the 10.0 mg/kg-day dose group on GD 20**

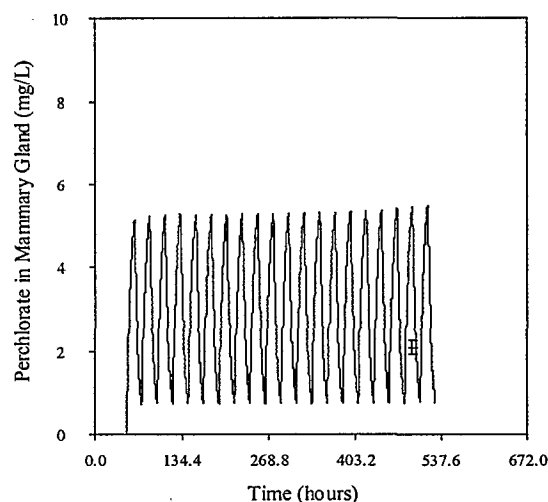


**Figure 11. Perchlorate concentration in the maternal mammary gland at the 10.0 mg/kg-day dose group on GD 20**

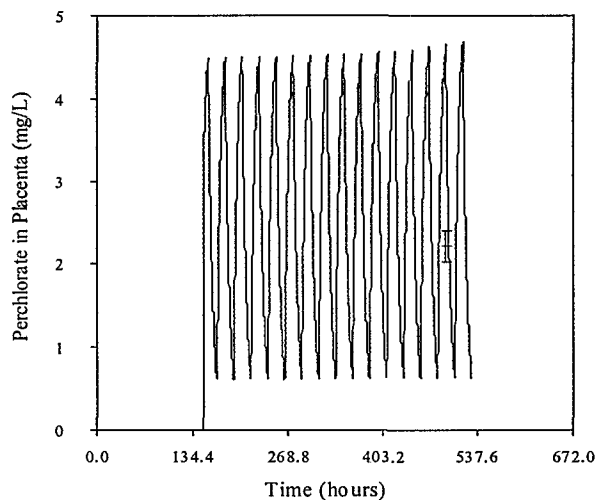


**Figure 12. Perchlorate concentration in the maternal placenta at the 10.0 mg/kg-day dose group on GD 20**

Due to the experimental difficulty involved in sampling the small fetal tissues, fewer data were available for perchlorate distribution in the fetus than in the dam. Figures 13 and 14 depict the model simulation of the fetal serum and skin levels compared to the data obtained in the drinking water study. Fetal serum and skin were pooled by litter.

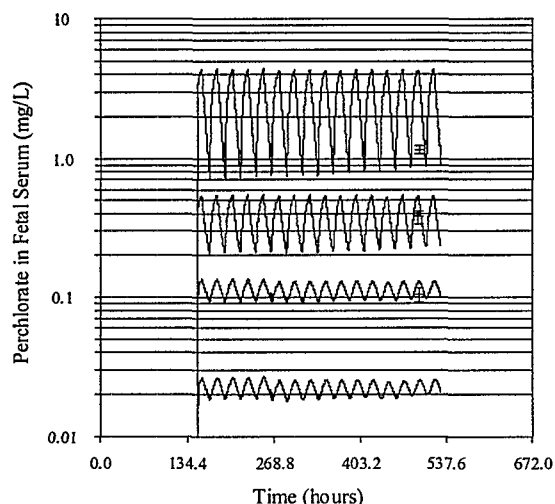


**Figure 13. Perchlorate concentration in the fetal serum at the 0.01, 0.1, 1.0 and 10.0 mg/kg-day dose groups on GD 20**

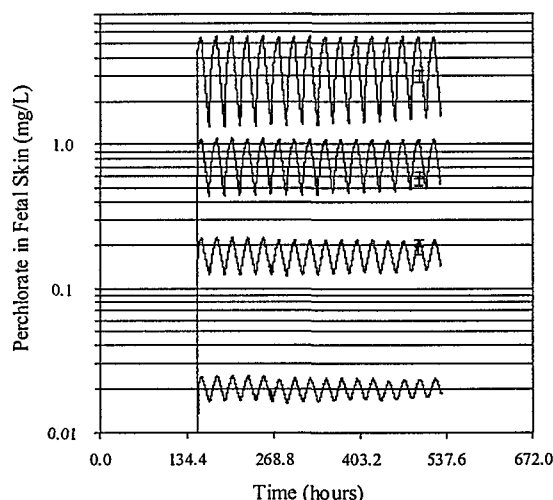


**Figure 14. Perchlorate concentration in the fetal skin at the 0.01, 0.1, 1.0 and 10.0 mg/kg-day dose groups on GD 20. Data from the 0.01 mg/kg-day group were below analytical detection.**

As described in the maternal tissues, the 10 mg/kg-day dose was used to determine the partition values in the fetal skin and GI tract. The lower doses were used to determine  $V_{max}$  values. Clearance values for transfer rates between the placenta and fetal serum were determined by fitting the model simulation to the fetal and maternal serum simultaneously, while keeping good fits in the other tissues. Drinking water data for the mixed GI tract and contents were available only in the 10 mg/kg-day dose group. The model simulation of the total gut (tract + contents) was therefore compared to the data for the total gut. Figure 15 shows the model simulation versus the total fetal gut perchlorate concentration.

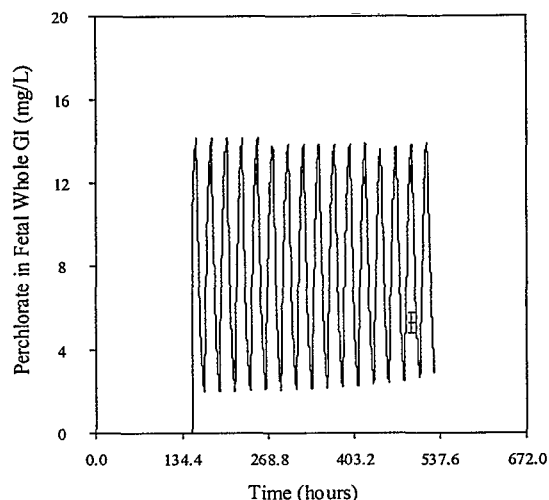


**Figure 15. Perchlorate concentration in the fetal gut at the 10.0 mg/kg-day dose group on GD 20**

**Iodide Parameterization.** Development of the iodide model was performed by fitting the model to the kinetic data in the tissues of the dam and fetus from the preliminary iodide study. Partitions and  $K_m$  values were available from literature and in-house male rat iodide kinetic data, as described previously. Therefore, only the values for  $V_{max}$  and  $PA$  needed to be fit with the model. The model simulation of the *iv* injection of 2.19 ng/kg  $^{125}I$  on GD 20 versus the experimental data is shown below. Figures 16 through 21 show the simulations for the various tissues measured in the pregnant rat. In these and subsequent plots, the cross-bars indicate the mean  $\pm$  one standard deviation.

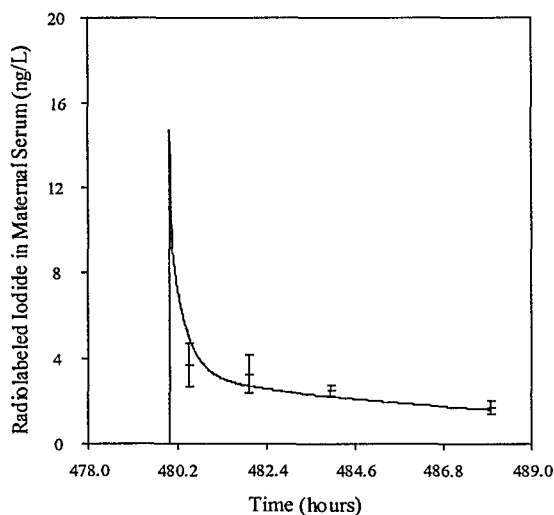


**Figure 16. Iodide Concentration in Maternal Serum after *iv* dose of 2.19 ng/kg  $^{125}I$**

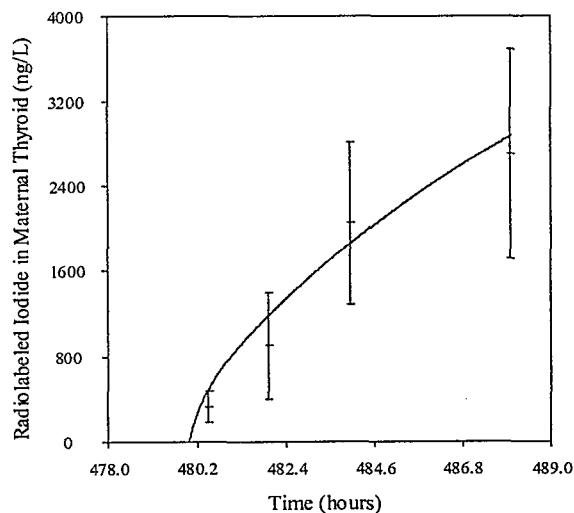


**Figure 17. Iodide Concentration in Maternal Thyroid after *iv* dose of 2.19 ng/kg  $^{125}I$**

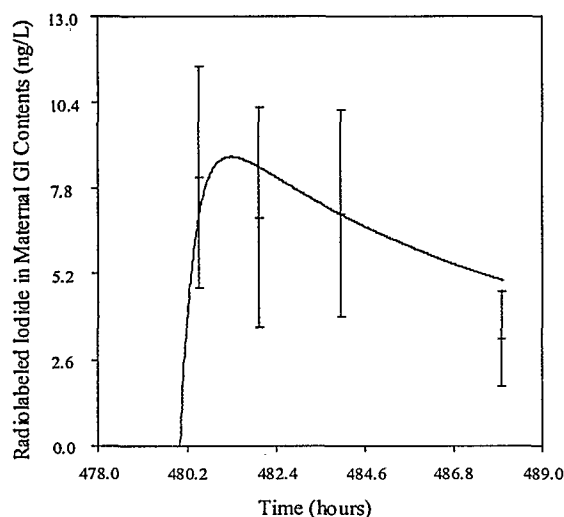


**Figure 18. Iodide Concentration in Maternal GI Contents after *iv* dose of 2.19 ng/kg  $^{125}\text{I}^-$**

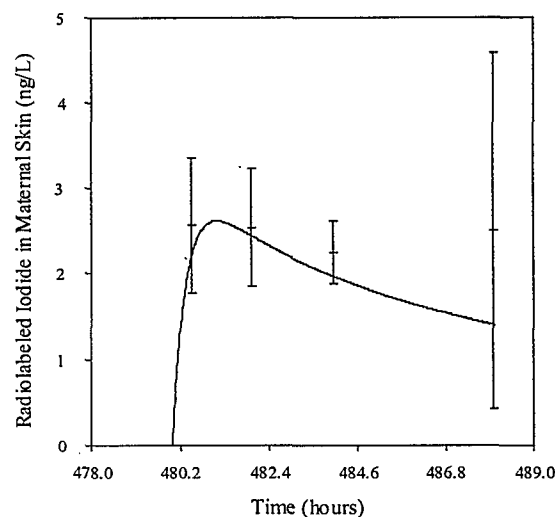


**Figure 19. Iodide Concentration in Maternal Skin after *iv* dose of 2.19 ng/kg  $^{125}\text{I}^-$**

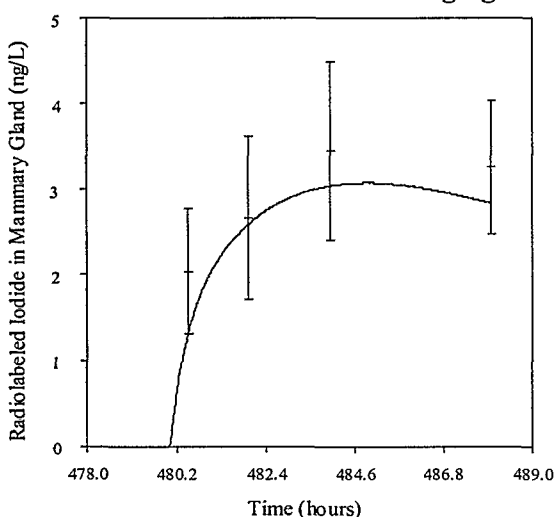


**Figure 20. Iodide Concentration in Mammary Gland after *iv* dose of 2.19 ng/kg  $^{125}\text{I}^-$**

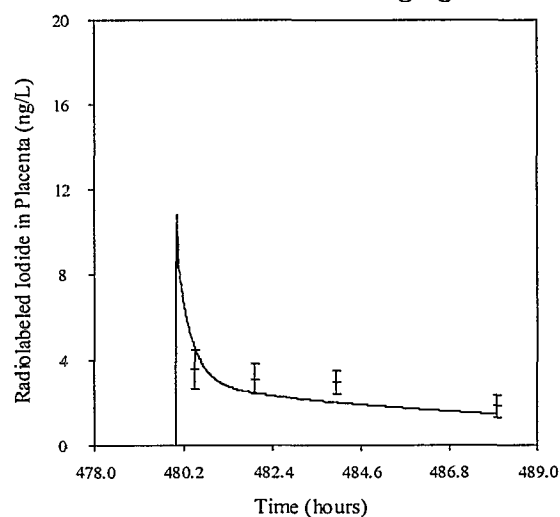


**Figure 21. Iodide Concentration in Placenta after *iv* dose of 2.19 ng/kg  $^{125}\text{I}^-$**

The model simulations describe the data well, using the literature and experimental parameters described in the Methods section. The clearance value for urinary excretion was determined by fitting the maternal serum prediction to the above data, while keeping good fits in the other tissues, such as the maternal skin and gut and the fetal skin. PA values were adjusted to describe the behavior of the iodide data, where varying the PA values toward 1.0 L/hr-kg generally increased the rate at which uptake and clearance in a particular tissue occurred, and decreasing PA slowed the uptake and clearance. The behavior of these mammary tissue data indicates that iodide is maintained in the mammary gland well into the clearance phase of the serum. In order to simulate this behavior, it was necessary to use a low PA value (0.02 L/hr-kg) in the mammary gland. The mammary:plasma ratios of greater than one were fit with the Vmax for mammary NIS. Clearance values for the transfer of iodide between the placenta and fetal blood were



determined by optimizing the fit of the fetal serum to the data points, while maintaining the fit of the simulations of the maternal blood and fetal tissue data. Figures 22 through 24 show the model simulation versus the fetal data in the preliminary iodide time course study.

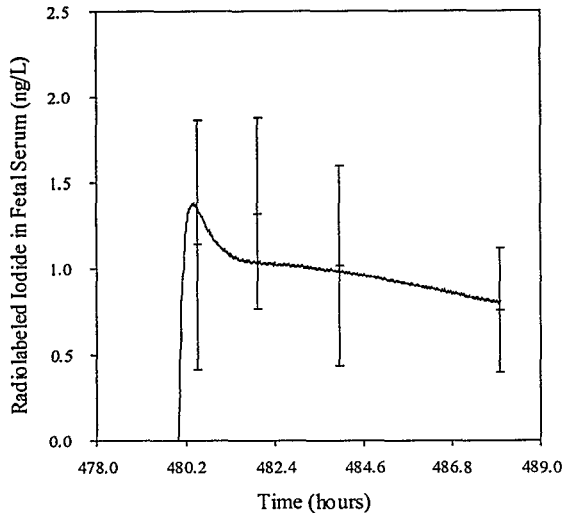


**Figure 22. Iodide Concentration in Fetal Serum after *iv* dose of 2.19 ng/kg  $^{125}\text{I}$  to the Dam**

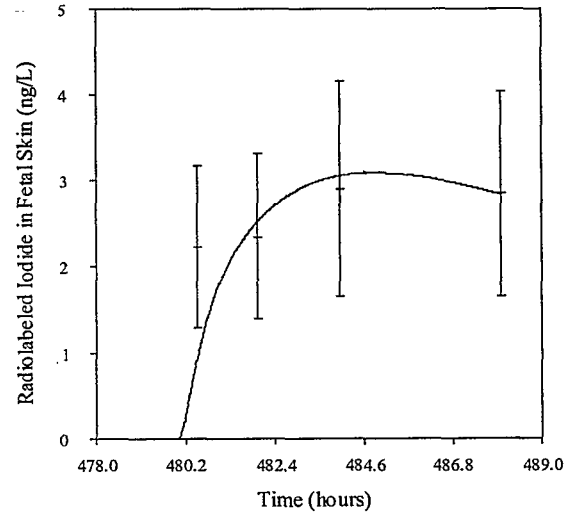


**Figure 23. Iodide Concentration in Fetal Skin after *iv* dose of 2.19 ng/kg  $^{125}\text{I}$  to the Dam**

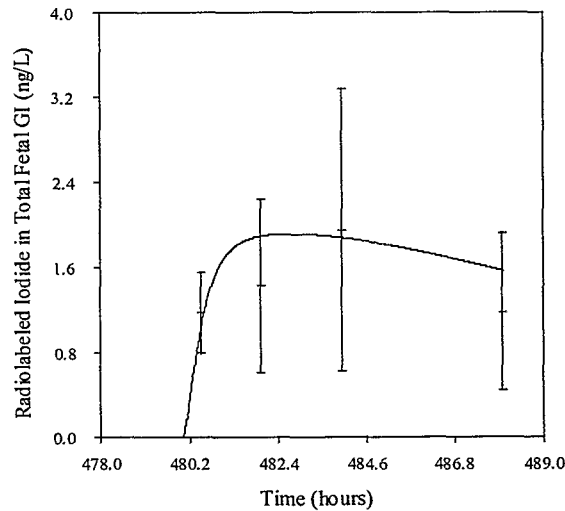


**Figure 24. Iodide Concentration in Total Fetal Gut after *iv* dose of 2.19 ng/kg  $^{125}\text{I}$  to the Dam**

Fetal GI content volumes were too small to be separated from fetal GI tract. Therefore, the model description of the total GI (tract + contents) was run against the fetal data. The behavior of the iodide in the fetal skin and GI were different from that seen in the dam. The iodide tended to stay in the tissue of the fetus longer, requiring a slower clearance in the fetal tissues than were used in the corresponding maternal tissue. As a result, lower PA values were used for the GI and

skin in the fetus versus those used in the dam. For example, the PA value in the skin was determined to be 0.1 L/hr-kg in the dam, but was decreased to 0.02 L/hr-kg in the fetus.

**Data of Feldman *et al.* (1961).** It has long been recognized that the fetal thyroid begins sequestering iodide on the 17<sup>th</sup> day of gestation. Fetal iodide uptake quickly increases through the final days of gestation (Carpenter, 1959; Feldman *et al.*, 1961). In order to account for the changing uptake in the fetal thyroid with the model, the simulation was fit to fetal thyroid data given in Feldman *et al.* (1961) on GD 17 through 19 of gestation. The values for Vmaxc\_Tfi were determined with the model. An equation (shown below) was fitted using an exponential curve to the values and the times given in Feldman *et al.* (1961), where t is the time of gestation in hours. This equation was then utilized in the model to account for the increasing ability of the fetal thyroid to incorporate iodide.

$$V_{maxc\_TFi} = 5.29 * 10^{-12} * (e^{0.0816t})$$

Figure 25 shows the model simulation for the amount of iodide in the fetal thyroid 24 hours after dosing on either GD 17, 18 or 19. GD 16 data were not used because the fetal thyroid is not yet sequestering iodide. Therefore, the values for Vmax are assumed to be 0.0 L/hr-kg in the model at GD 16. From the data, iodide levels were negligible in the fetal thyroid on day 16. Only the mean of the measured data was given in Feldman *et al.* (1961). Therefore, standard deviations are not shown on the plot.

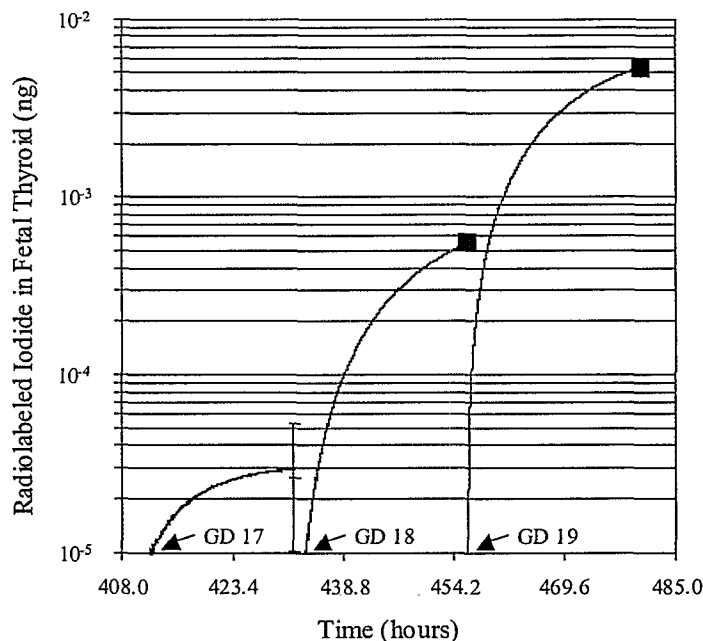


**Figure 25. Amount of Iodide in the fetal thyroid 24 hours after exposure on GD 17, 18 and 19 (Feldman *et al.*, 1961). Cross-bar indicates the range of data, squares indicate the reported averages**

## Model Validation

**Perchlorate Induced Iodide Inhibition.** The inhibition of iodide uptake into the thyroid and the resulting effect on the maternal and fetal serum was simulated against the data collected during the in-house inhibition study on GD 20. The kinetic parameters derived from the perchlorate drinking water and preliminary iodide data sets were used in the model simulation. Since the inhibition study was performed with an acute perchlorate dose, it was necessary to make some slight changes in the thyroid perchlorate kinetics. The long-term exposure to perchlorate in the drinking water studies (18 days), which were used to determine the perchlorate parameters, is sufficient to induce up-regulation in the thyroid (Yu *et al.*, 2000a). Therefore, the thyroid parameters in the dam at this point would be different from those seen in an acute situation. The only parameters altered in order to model the acute perchlorate were the partition coefficient (from 2.25 to 0.13) and PA value (from  $6.0\text{E-}4$  to  $9.0\text{E-}5$ ) into the thyroid at the basolateral membrane (thyroid follicle). The value for the partitioning into the follicle in a naïve thyroid was calculated as described previously from Chow and Woodbury (1970). The PA value in the naïve thyroid follicle was determined with the lactation model, which is described in another paper (Clewett *et al.*, 2001). The model simulation was fit to the available kinetic data in the thyroid, while keeping all other thyroid parameters identical to those in the pregnancy model. Figure 26 illustrates the model prediction of thyroidal iodide uptake with and without perchlorate inhibition, utilizing the pre-set parameters.

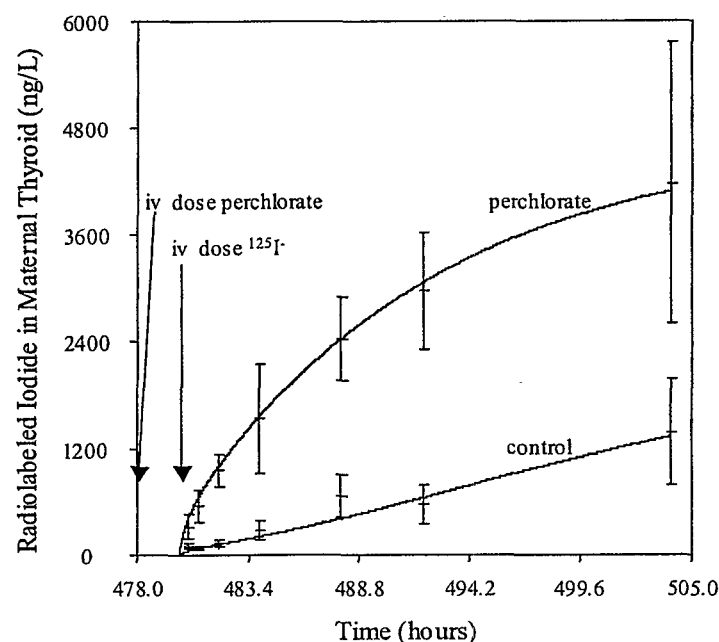


**Figure 26. Iodide Concentration in Maternal Thyroid with and without 1.0 mg/kg  $\text{ClO}_4^-$  *iv* dose 2 hours prior to an *iv* dose of 1.87 ng/kg  $^{125}\text{I}^-$  to the Dam. The top simulation (solid line) indicates the control thyroid. The lower simulation and data indicate the inhibited thyroid.**

As can be seen in Figure 26, the model simulation of inhibition in the thyroid gland at 0.5, 1., 2, 4, 8, 12 and 24 hours after dosing with iodine shows an excellent fit to the data. The use of parameters derived from the drinking water perchlorate data for acute kinetics is well supported by the inhibition of iodide, because inhibition is highly dependent on the perchlorate concentration in the thyroid and the perchlorate affinity constants in the apical and basolateral membranes of the thyroid. Figures 27 and 28 illustrate the effect of perchlorate thyroid inhibition on the maternal and fetal blood levels. Significant differences were found in the maternal serum iodide concentrations collected at the 1, 4 and 24 hour time points. Fetal serum, however, did not show any significant differences in the total serum iodide between the control and inhibited groups. Attachment 2 provides a summary of the statistical analysis of this data set.

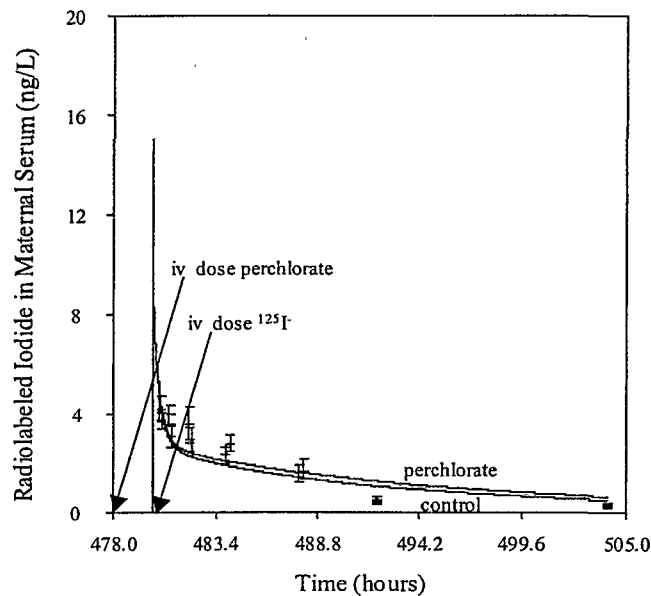


**Figure 27. Iodide Concentration in Maternal Serum with and without 1.0 mg/kg  $\text{ClO}_4^-$  *iv* dose 2 hours prior to an *iv* dose of 1.87 ng/kg  $^{125}\text{I}^-$  to the Dam. The top simulation (solid line) and data (cross bars) indicate the serum during thyroid inhibition. The lower simulation and data indicate the control serum.**

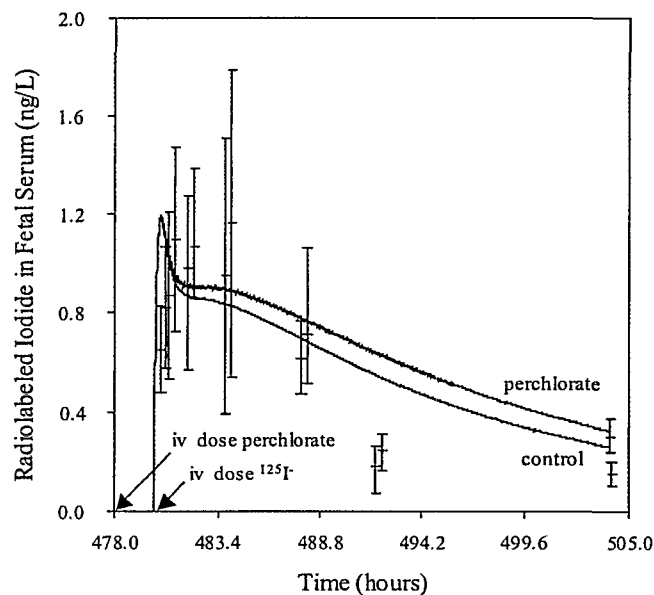


**Figure 28. Iodide Concentration in Fetal Serum with and without 1.0 mg/kg  $\text{ClO}_4^-$  *iv* dose 2 hours prior to an *iv* dose of 1.87 ng/kg  $^{125}\text{I}^-$  to the Dam. The top simulation (solid line) and data (cross bars) indicate the fetal serum during maternal thyroid inhibition. The lower simulation and data indicate the control serum.**

Although most of the data are not statistically different for the serum between the control and inhibition groups, there is an evident trend in which both the maternal and fetal serum iodide levels increase. The model describes this same trend, showing increased serum iodide levels resulting from acute perchlorate exposure. Since only the thyroid was modeled with inhibition, the increased serum iodide levels are entirely a result of decreased ability of the thyroid to sequester iodide.

**Data of Versloot *et al.* (1997).** A simulation of data presented by Versloot *et al.* (1997) after an injection of 10  $\mu\text{Ci}$  (or 1.74 ng/kg) carrier free  $^{125}\text{I}$  in GD 19 dams was performed with the model in order to test the model to predictions of diverse data sets collected under different conditions than the data used in parameterization. Previous data sets used in model development were only available for GD 20. This data set provided an additional time point for the iodide model validation (GD 19). Versloot and coauthors were able to measure the amount of iodide taken up in the fetal thyroid. The collection and analysis of fetal thyroid were not available in any previous data sets in spite of the fact that the fetal thyroid, along with the maternal thyroid, is a major tissue of interest in developmental effects. Figures 29 through 33 depict the model simulation compared to the experimental data in the maternal thyroid, mammary gland, placenta, fetal thyroid and fetal carcass after removal of the thyroid.

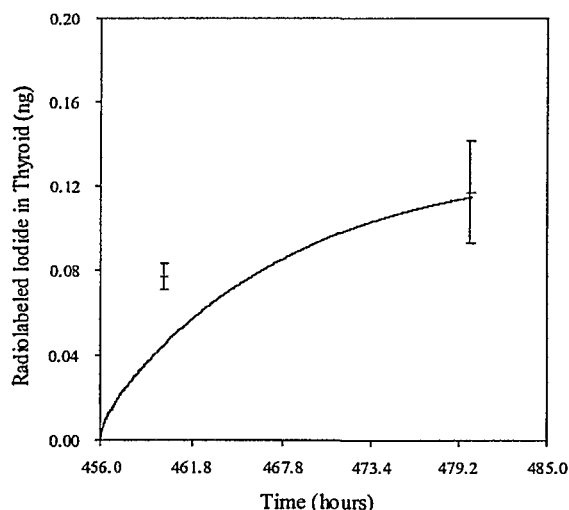


**Figure 29. Total Amount of Iodide in Maternal Thyroid.** The model simulation is shown versus the mean  $\pm$  SD at the 4 and 24 hour data points after exposure on GD 19 (Versloot *et al.*, 1997).

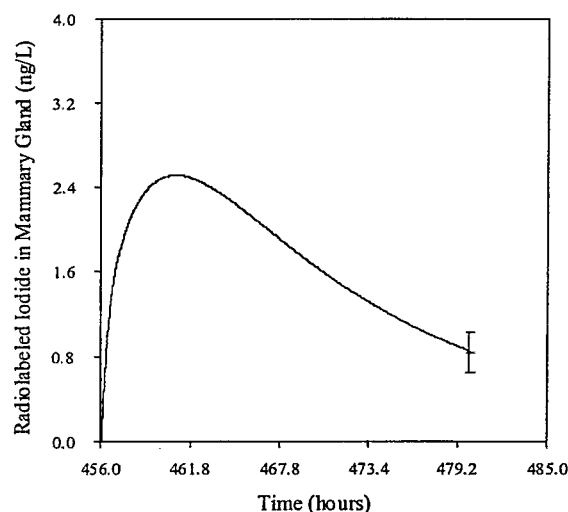


**Figure 30. Iodide Concentration in the Mammary Gland.** The model simulation is shown versus the mean  $\pm$  SD of the data, 24 hours after exposure on GD 19 (Versloot *et al.*, 1997).

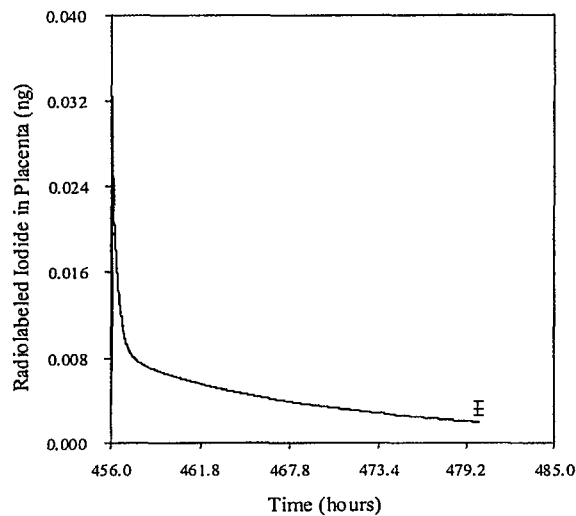


**Figure 31. Amount of Iodine in the Placenta. The model simulation is shown versus the mean  $\pm$  SD of the data at 24 hours after exposure on GD 19 (Versloot *et al.*, 1997).**

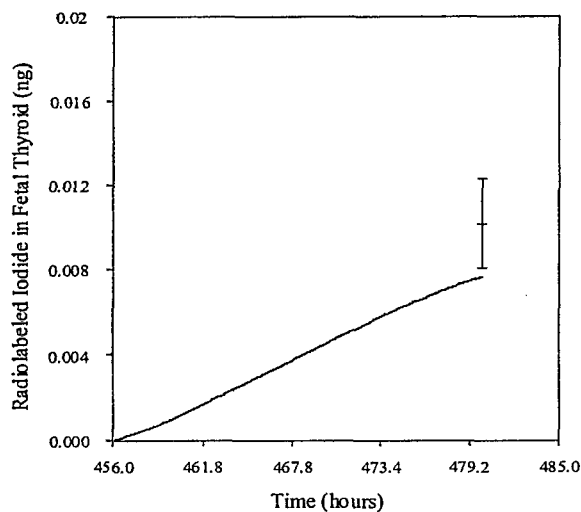


**Figure 32. Total Amount of Iodine in the Fetal Thyroid. The model simulation is shown versus the mean  $\pm$  SD of the data at 24 hours after exposure on GD 19 (Versloot *et al.*, 1997).**

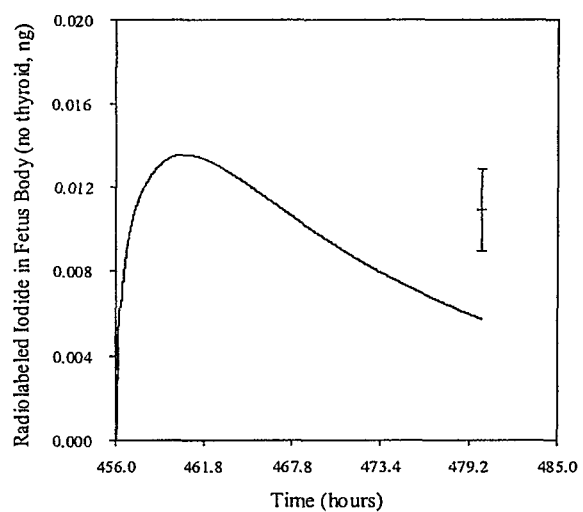


**Figure 33. Total Amount of Iodine in Fetal Carcass without Thyroid. The model simulation is shown versus the mean  $\pm$  SD of the data at 24 hours after exposure on GD 19 (Versloot *et al.*, 1997).**

The ability of the model to predict the GD 19 data collected by Versloot *et al.* (1997) in Wistar rats was verified with the tissues fitted previously on GD20 and the fetal thyroid and fetal carcass after removal of the thyroid. The model prediction of the total body burden under-predicted the rest of body iodine content in the fetus after removal of the thyroid. It appears that the loss of iodine is slightly over-estimated in the fetus. However, the model simulation is within a factor of two from the data. The model was able to reproduce the data from the other tissues without changing any of the previously described parameters. The ability of the model to simulate data from a study performed on a different gestation day from a separate laboratory, without changing

any parameters, is quite remarkable. Additionally, the 24 hour time point was not available in the data used for model parameterization, except in the case of the fetal thyroid. The model, therefore, was able to predict data at a time point not previously tested.

**Data of Sztanyik and Turai (1988).** A simulation of data reported in Sztanyik and Turai (1988) after an injection of 370 kBq (or 0.36 ng/kg) carrier free  $^{131}\text{I}$  in GD 20 dams was performed with the model in order to further test the predictive capability of the model. Previous data sets used in model development and validation were all taken at similar dose levels (1.74 to 2.42 ng/kg I) and with  $^{125}\text{I}$ . This data set provided an additional dose level and a second species of radiolabeled iodide for the model validation. Figures 34 and 35 show the model simulation compared to the experimental data in the placenta and the total amount in the fetus.

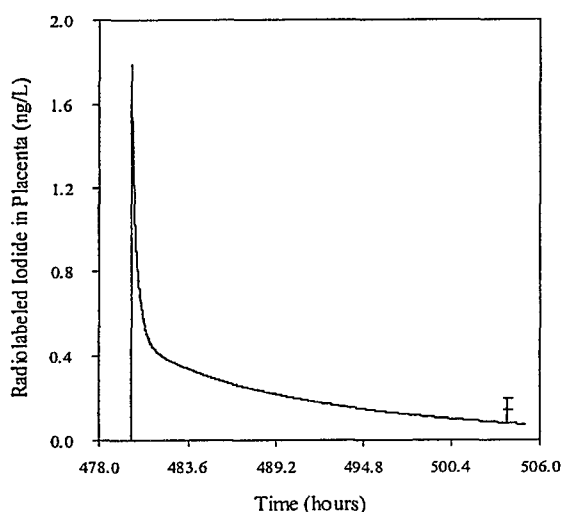


**Figure 34. Iodide Concentration in the Placenta.** The model simulation is shown versus the mean  $\pm$  SD of the data at 24 hours after exposure on GD 20 (Sztanyik and Turai, 1988).

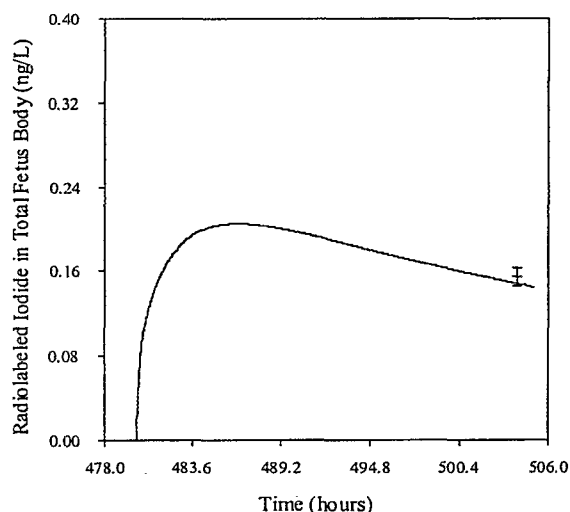


**Figure 35. Concentration of Iodide in the Whole Body of the Fetus.** The model simulation is shown versus the mean  $\pm$  SD of the data at 24 hours (Sztanyik and Turai, 1988).

The model was again able to reproduce the data well. Simulations again showed acceptable fits to the 24-hour time point. No parameters were changed from the originally assigned values.

**Drinking Water Inhibition Data.** Iodide inhibition and the corresponding behavior in the several other maternal and fetal tissues were measured by AFRL/HST after maternal exposure to perchlorate in drinking water at doses of 0.0, 0.01, 0.1, 1.0 and 10.0 mg/kg-day for 18 days. None of the tissues measured after 18 days of perchlorate dosing show significant differences from control values. However, the control data are useful for validation of the model at dose levels that are more than four orders of magnitude greater than the dose used in model



parameterization (33000 ng/kg versus 2.19 ng/kg). Figures 36 through 41 illustrate the model prediction of various tissues in the dam and fetus on GD20.

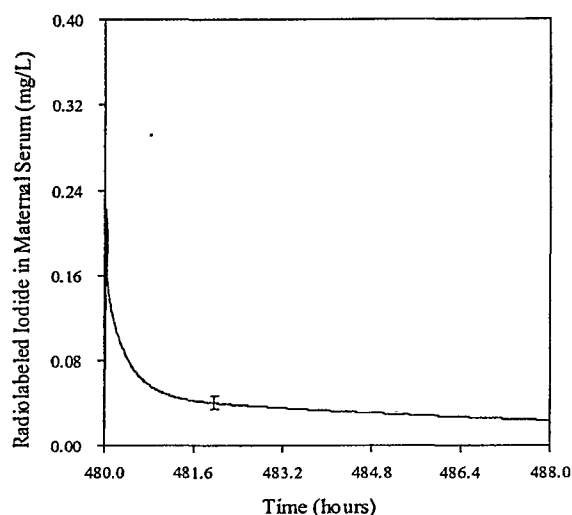


**Figure 36. Iodide Concentration in Maternal Serum 2 hours after *iv* dose of 33000 ng/kg  $^{125}\text{I}$  with carrier**

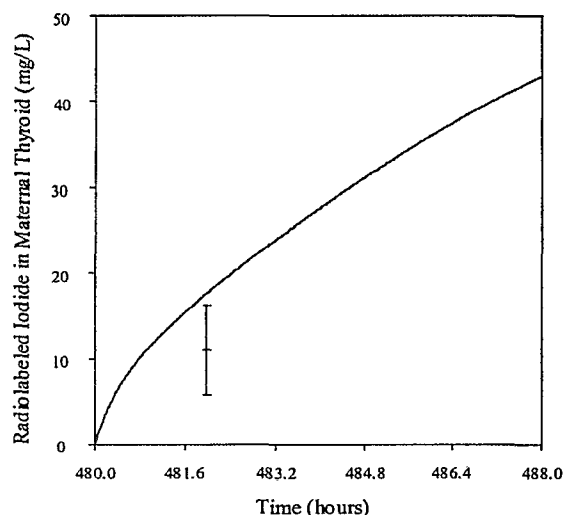


**Figure 37. Iodide Concentration in Maternal Thyroid 2 hours after *iv* dose of 33000 ng/kg  $^{125}\text{I}$  with carrier**

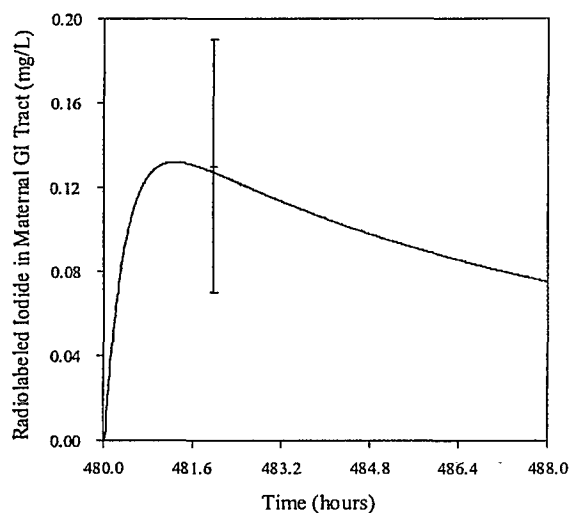


**Figure 38. Iodide Concentration in Maternal GI Tract 2 hours after *iv* dose of 33000 ng/kg  $^{125}\text{I}$  with carrier**

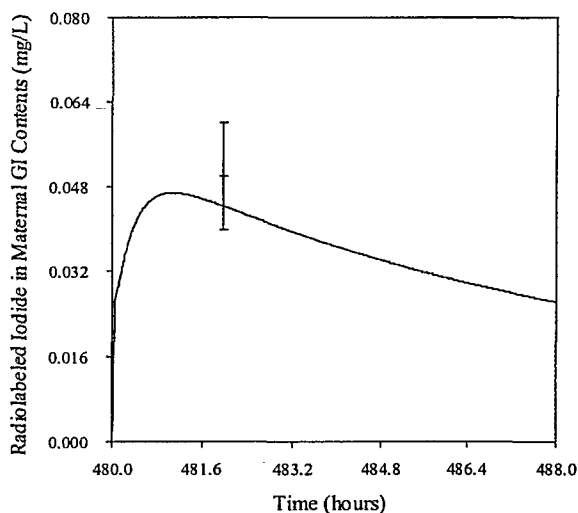


**Figure 39. Iodide Concentration in Maternal GI Contents 2 hours after *iv* dose of 33000 ng/kg  $^{125}\text{I}$  with carrier.**

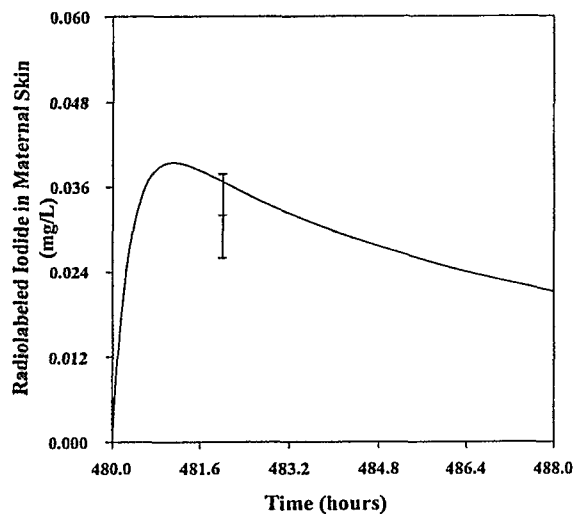


**Figure 40. Iodide Concentration in Maternal Skin 2 hours after *iv* dose of 33000 ng/kg  $^{125}\text{I}$  with carrier**

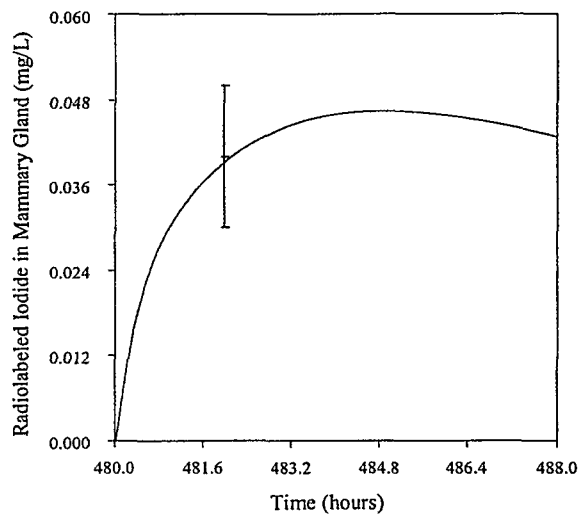


**Figure 41. Iodide Concentration in Mammary Gland 2 hours after *iv* dose of 33000 ng/kg  $^{125}\text{I}$  with carrier**

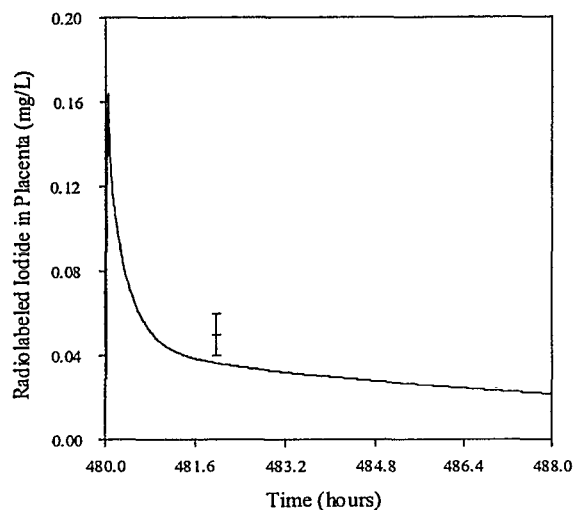


**Figure 42. Iodide Concentration in Placenta 2 hours after *iv* dose to dam of 33000 ng/kg  $^{125}\text{I}$  with carrier**

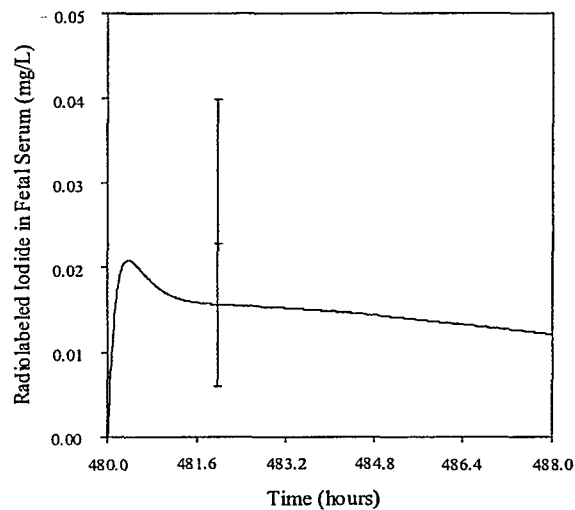


**Figure 43. Iodide Concentration in Fetal Serum 2 hours after *iv* dose to dam of 33000 ng/kg  $^{125}\text{I}$  with carrier**

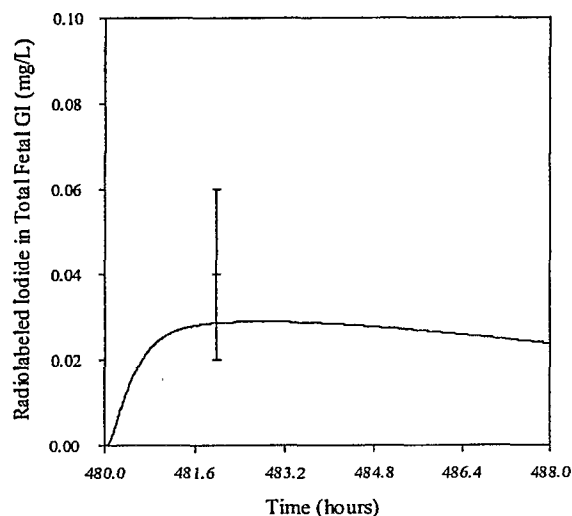


Figure 44. Iodide Concentration in Fetal GI 2 hours after *iv* dose to dam of 33000 ng/kg  $^{125}\text{I}^-$  with carrier

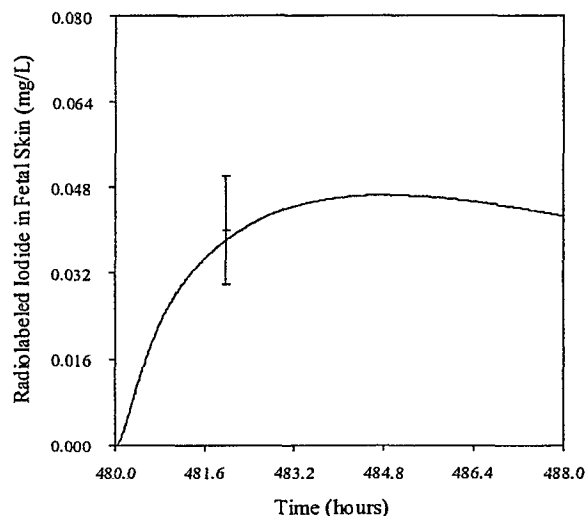


Figure 45. Iodide Concentration in Fetal Skin 2 hours after *iv* dose to dam of 33000 ng/kg  $^{125}\text{I}^-$  with carrier

The inhibition data collected after maternal exposure to perchlorate contaminated drinking water presented interesting changes in the kinetics of iodide. As is expected, the introduction of perchlorate into the drinking water causes an initial inhibition of the thyroidal iodide uptake, which then results in a systemic response resulting in up-regulation of the thyroid. Although data were not collected to verify the initial iodide inhibition, it is evidenced by the subsequent changes in hormones. The following tables summarize the hormone changes seen in the GD 20 dam (Table 4) and fetus (Table 5) after 18 days of exposure to 0.1, 1.0 and 10.0 mg/kg day  $\text{ClO}_4^-$  doses, expressed as change from control.

TABLE 4. PERCENT CHANGE IN THYROID HORMONES OF PREGNANT RAT AFTER PERCHLORATE EXPOSURE

Perchlorate Dose (mg/kg-day)	Total $\text{T}_4$ (% change)	Free $\text{T}_4$ (% change)	Total $\text{T}_3$ (% change)	TSH (%change)
0.01	-32***	5	-3	33***
0.1	-35***	51***	-6	37***
1.0	-39***	83***	-9*	69***
10.0	-47***	95***	-12**	115***

**TABLE 5. PERCENT CHANGE IN THYROID HORMONES OF FETUS AFTER  
PERCHLORATE EXPOSURE**

<b>Perchlorate Dose (mg/kg-day)</b>	<b>Total T<sub>4</sub> (% change)</b>	<b>Free T<sub>4</sub> (% change)</b>	<b>Total T<sub>3</sub> (% change)</b>	<b>TSH (%change)</b>
<b>0.01</b>	-2	3	-3	12
<b>0.1</b>	-8	18*	-4	17*
<b>1.0</b>	-15*	19*	-8	30***
<b>10.0</b>	-17**	60***	-10	48***

\* 0.01 < p ≤ 0.05

\*\* 0.001 < p ≤ 0.01

\*\*\* p ≤ 0.001

From the results shown in the tables above, it is apparent that even at the lowest dose, the hormonal system has experienced a perturbation and is attempting to compensate for the interruption caused by the perchlorate exposure. Maternal T<sub>4</sub> is shown to decrease in a dose-dependent manner, while TSH increases dose-dependently. Maternal Total T<sub>4</sub> and TSH changes are statistically significant at all doses. Free T<sub>4</sub> is significantly increased at the 0.1, 1.0 and 10.0 mg/kg-day doses and Total T<sub>3</sub> is significantly decreased at the 1.0 and 10.0 mg/kg-day doses. The fetus appears to follow the same trends as those seen in the dam. However, only the 1.0 and 10.0 mg/kg-day dose groups show significant decreases in Total T<sub>4</sub> and the 0.01, 1.0 and 10.0 mg/kg-day doses result in significant increases in fetal Free T<sub>4</sub> and TSH. No significant decrease was seen in fetal T<sub>3</sub>. Hormone changes are discussed in detail elsewhere (Yu *et al.*, 2000a). The statistical analysis of the hormone data is attached (Attachment 3).

From the perspective of iodide kinetics, these hormone changes are important indicators of thyroid up-regulation. When TSH is increased, the thyroid is stimulated to increase iodide uptake. It is evident, then, that after exposure to perchlorate in drinking water for 18 days, the thyroid of the pregnant dam has experienced both inhibition and up-regulation and has successfully compensated for the competition of perchlorate for binding sites of NIS. Therefore, it is not surprising that no inhibition was reported on GD 20. It is not that the inhibition is not taking place, but rather that the system has compensated for the effect of perchlorate. The thyroid of the dam was able to increase iodide uptake to restore thyroidal iodide uptake to normal levels. Table 6 shows the iodide levels measured in the tissues from the GD 20 drinking water study. The protocol for this study is discussed further in Yu *et al.* (2000a).

**TABLE 6. MEAN IODIDE UPTAKE IN TISSUES AFTER 28 DAYS OF  
PERCHLORATE EXPOSURE**

<b>Maternal Tissues</b>	<b>Control</b>	<b>0.01 ClO<sub>4</sub><sup>-</sup></b>	<b>0.1 ClO<sub>4</sub><sup>-</sup></b>	<b>1.0 ClO<sub>4</sub><sup>-</sup></b>	<b>10.0 ClO<sub>4</sub><sup>-</sup></b>
Serum (mg/L)	0.04	0.05	0.05	0.06	0.06
Thyroid (mg/L)	11.06	14.97	10.48	11.48	10.47
GI Content (mg/L)	0.13	0.12	0.11	0.12	0.09
GI Tract (mg/L)	0.05	0.04	0.05	0.06	0.05
Skin (mg/L)	0.03	0.03	0.04	0.04	0.04
Mammary (mg/L)	0.04	0.03	0.03	0.03	0.04
Placenta (mg/L)	0.05	0.04	0.05	0.03	0.03
<b>Fetal Tissues</b>					
Serum (mg/L)	0.02	0.02	0.03	0.03	0.02
Total GI (mg/L)	0.04	0.06	0.08	0.07	0.04
Skin (mg/L)	0.04	0.04	0.04	0.03	0.02

The model is not equipped with the capability to account for up-regulation of the thyroid. Therefore, when a simulation of the inhibition is performed with the model, the concentration of iodide is under-predicted in a (ClO<sub>4</sub><sup>-</sup>) dose-dependent manner. Figure 46 shows the model prediction of iodide in the thyroid of the dam at drinking water doses of 0.0, 0.1, 1.0 and 10.0 mg/kg-day. The Vmax for iodide was decreased to  $2.5 \times 10^4$  to fit the mean from the control data with the control simulation, in order to make the comparison of the inhibition data and simulations clearer. All experimental data were actually taken at two hours post-dosing. However, the data points were separated slightly by time on the plot in order to make them more visible. The model's prediction of thyroid perchlorate levels from this same study can be seen in Figure 7.

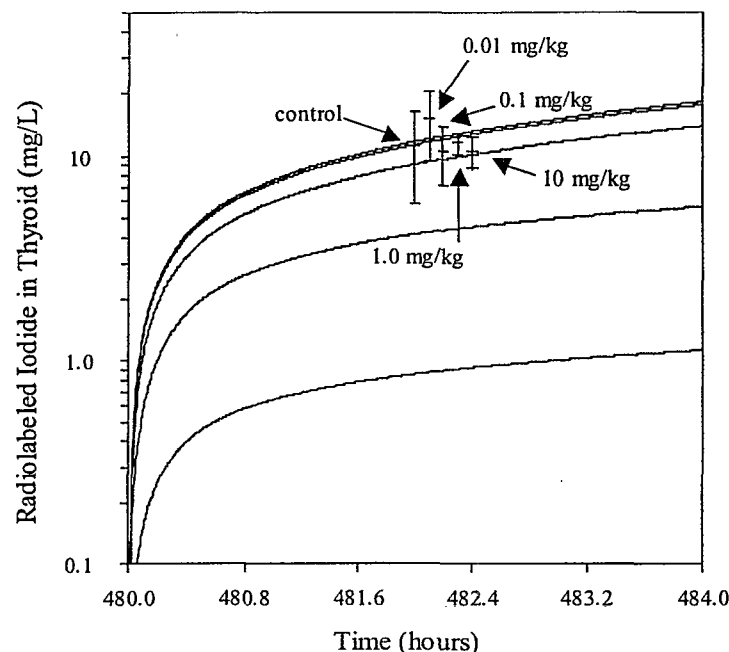


**Figure 46. Iodide in Thyroid on GD 20 after 18 days of 0.0, 0.1, 1.0 and 10.0 mg/kg-day  $\text{ClO}_4^-$  in drinking water. Solid lines are model simulations and cross-bars are the mean  $\pm$  SD of data.**

## CONCLUSION

Throughout the process of model development, it was evident that several differences exist between the pregnant female and male rats. The differences seen between this model and the male rat model that was developed concurrently by Merrill *et al.* (2001a) emphasized the need for a pregnancy model to describe a highly dynamic, changing system. Beyond the more obvious physiological changes occurring during pregnancy, some differences exist that affect the kinetics of both perchlorate and iodide. The thyroidal maximum capacities are lower in the pregnant dam than in the male rat. Model parameterization in the male rat indicated the need for  $V_{\text{max}}$  values for uptake into the follicle of the thyroid of  $2.2 \times 10^3$  L/hr-kg for perchlorate and  $5.5 \times 10^4$  L/hr-kg for iodide, while the gestation model required values of  $1.8 \times 10^3$  L/hr-kg and  $4.0 \times 10^4$  L/hr-kg for the same parameters. This difference is supported in the literature. Versloot *et al.* (1997) suggest that the pregnant rat may have a lowered reserve of iodide in the thyroid toward the end of pregnancy, causing increased activity in the thyroid. The increased response of the pregnant rat was also seen in the studies performed by Yu *et al.* (2000a and 2000b), which reported a greater than average inhibition in the thyroid of the pregnant dam than in the male rat at the same  $\text{ClO}_4^-$  dose (78% vs. 70% over 8 hours). The skin of the pregnant dam also required a smaller value for  $V_{\text{max}}$  than the male rat. This is supported by the work of Brown-Grant and Pethes (1959), who reported higher levels of iodide in the skin male rats than in female rats. Skin, therefore, appears to be a more important iodide reserve in the male rat than the female. It is not surprising that the kinetic behavior of perchlorate and iodide would vary somewhat between a male rat and a pregnant female rat. In fact, it is quite remarkable that the

model is able to account for the majority of differences in the uptake, distribution and excretion between the male and pregnant female by incorporating known differences in physiology.

The described PBPK gestation model is able to predict the distribution of perchlorate in the tissues of active uptake and serum of the pregnant dam and fetus on GD 20 after exposure to perchlorate in drinking water. Perchlorate distribution in this dynamic system is well described utilizing a pharmacokinetic approach to the modeling and accounting mathematically for physiological changes, such as changing tissue volumes and maternal and fetal growth. The model predicts the transfer of perchlorate to the fetus and is also able to describe the uptake into fetal tissues of interest, such as the skin. Fetal and dam tissues are simulated by fitting data that ranges from 0.01 to 10.0 mg/kg-day, or three orders of magnitude.

At this time very little data are available on perchlorate kinetics in the pregnant rat. Although perchlorate has been used extensively in literature to study the thyroidal uptake of iodide, it has not been commonly used in rat gestation studies. As such, the perchlorate model is limited to utilizing the drinking water studies for parameterization. However, acute kinetic data were available for perchlorate in the lactating dam and were utilized in the development of the rat lactation model (Clewell *et al.*, 2001). This system is similar to that of the pregnant dam and it was possible to simulate the perchlorate kinetics of the dam with the same general model structure, changing only the physiological parameters. Therefore, it seemed reasonable to use the acute perchlorate parameters from the lactation model. The use of the described parameters for acute perchlorate kinetics is also supported by the ability of the model to predict inhibition in the pregnant dam. Acute perchlorate kinetic data to further verify the model are currently being analyzed by AFRL/HEST. In these studies, tissues were collected from pregnant dams and fetuses at various time points after *iv* injections of perchlorate.

The kinetic behavior of iodide in the complex system of a pregnant rat and fetus was also accurately simulated with a range of doses that spans nearly five orders of magnitude (0.36 to 33,000 ng/kg). The active sequestration of iodide in maternal and fetal tissues and the transfer of iodide between mother and fetus was described kinetically with the model and data have been simulated at a variety of doses and at various time points up to 24 hours after exposure. The fact that the model was able to simulate data from other laboratories under a variety of different conditions attests to the validity of the model structure and its applicability to other studies. The purpose of developing a PBPK model is to aid in predicting the effect of exposure in situations that are not easily or already measured. The usefulness of this model for this purpose is supported by the success the model has already had in reproducing literature studies.

The ability of the model to predict iodide was indicative of the usefulness of the model for predictive purposes. It was possible to predict inhibition out to 24 hours, while simulating the serum and thyroid perchlorate and iodide levels with satisfactory accuracy. This provides support for the chosen model structure, as well as validation for the physiological and chemical descriptions used. However, it is important to note that in the majority of the situations of interest, the exposure to perchlorate would very likely be through the ingestion of contaminated drinking water. In this scenario, the endocrine system is given plenty of time to undergo up-regulation. Therefore, the inability of the model to respond to this auto-regulation presents a considerable need for further model development.

Hormone homeostasis is a complex process and is not included in the present model structure. Predicting results from experiments such as the drinking water study would require a model that could account for the hormone levels in tissues and serum and processes such as hormone production, storage and secretion in the thyroid, conversion of  $T_4$  to  $T_3$  in the tissues, deiodination of  $T_4$  and  $T_3$  to less active forms and a feedback mechanism between the hormone levels and thyroid symporter. Our laboratory is currently working toward this goal, viewing the current modeling of iodide kinetics as the first step in the more complex modeling of hormone regulation by the pituitary-iodide axis. Kohn *et al.* (1996) has recently developed a PBPK model that attempts to describe the effect of dioxin on thyroid hormones. Although perchlorate and dioxin act on the endocrine system through different modes of action, it is likely that a similar approach to that of Kohn *et al.* could be employed for the hormone feedback system in the case of perchlorate.

The ultimate purpose of PBPK modeling in the evaluation of exposure risk is to predict the effect in the human population. This is also the aim of the perchlorate modeling effort. A perchlorate PBPK model for the adult male human has been developed simultaneously with the model described in this report. However, it is evident that large differences exist between the average human and the pregnant female rat, both physiologically and kinetically. The differences seen during the concurrent modeling effort in the male and pregnant female rat highlight the need for a human gestational model. The next stage, then, for this rat gestational model is to endeavor to use the model for human predictions. In order to attempt this, the model described in this paper will be equipped with human physiological parameters, such as human fetal growth. The model would then be run with the present kinetic parameters in an effort to predict the behavior of iodide and perchlorate in a pregnant human. It is possible that some of the chemical specific parameters will vary from the previously determined rat parameters. For example, Merrill *et al.* (2001b) found that the thyroidal capacity for iodide in humans is much higher than rats. However, as is evidenced by a comparison of the male rat and human perchlorate models (Merrill *et al.* 2001a and Merrill *et al.* 2001b) the physiological changes should account for the majority of the differences between the rat and human kinetics, with the present model structure. The application of this gestation model to human pregnancy will be described in future publications.

Ultimately, the gestation model could be a useful tool in determining the dosimetry for specific time points in gestation. These internal dosimetrics could then be compared to periods in which perchlorate exposure and/or iodide deficiency has been linked to developmental effects. It is difficult, however, to experimentally determine the specific times at which the availability of iodide to the fetus is most critical. Although the studies performed to this end are numerous, it is difficult to separate the pre- and postnatal effects of iodide deficiency, due to the fact that many effects are not manifested until later in life (e.g., lowered IQ). It has been suggested that in humans, the thyroid hormones are of little importance in early fetal life but are more critical during late fetal life in skeletal development and possibly in brain development, due to the fact that myelination takes place a few weeks before birth. However, since human effects are not easily recognized or measured at birth, it is difficult to say with certainty that this is the case. Developmental effects have been studied extensively in animal development, particularly in the rat. However, when using the rat as a species of comparison, the issue is further complicated by



the fact that rats are born in a more immature state than human infants. Therefore, much of the development that would take place *in utero* in the human is experienced during the lactation period of the rat (Myant, 1971).

It is conceivable that the PBPK models could be used to help determine the answers to these questions concerning the critical time points and major routes of exposure during development. The models could also be a useful tool to help ferret out whether exposure is more critical during the gestation or lactation. A lactation exposure model has also been developed for perchlorate and iodide in the lactating rat (Clewell *et al.*, 2001) utilizing the same approach, general compartmental structure and kinetic parameters as those seen in the gestation model. The physiological differences between lactation and pregnancy are addressed mathematically within in the structure of the model. These models, when used together, could provide a complete picture of the developmental period. It would be possible to utilize the models to predict dosimetry for specific time points during gestation and lactation, which could then be compared to studies in which developmental effects were identified. Thus the ultimate goal of the lactation and pregnancy models would be to utilize the models to compare exposure scenarios between the rat and human at different developmental time points, in order determine the dose and timing responsible for reported developmental effects.

#### ACKNOWLEDGEMENTS

The animals used in in-house studies were handled in accordance with the principles stated in the *Guide for the Care and Use of Laboratory Animals*, National Research Council, 1996, and the Animal Welfare Act of 1966, as amended.

The authors would like to thank Tammie Covington and Harvey Clewell for their aid in implementation of the gestational growth. A special thanks is extended to Latha Narayanan and Gerry Buttler for the sample analyses. The authors would also like to thank Dick Godfrey, Peggy Parish, SSgt Todd Ligman, TSgt Jim McCafferty, Tim Bausman, SSgt Paula Todd and TSgt Rick Black for their work with the gestation studies. The authors would also like to acknowledge Charles Goodyear for performing statistical analyses of the data. Mr. Goodyear is a statistical consultant for AFRL, Human Effectiveness Directorate, Crew Systems Interface Division (AFRL/HEC), Wright-Patterson Air Force Base, Ohio.

#### REFERENCES

- Ajjan, R.A.; Kamaruddin, N.A.; Crisp, M.; Watson, P.F.; Ludgate, M.; Weetman, A.P. (1998). Regulation and tissue distribution of the human sodium iodide symporter gene. *Clin. Endocrinol.*, 49 (4), p. 517-523.
- Altman, P.L., and Dittmer, D.S. (1971). Volume of blood in tissue: Vertebrates: (148):p. 383-387. Respiration and Circulation. Federation of American Societies for Experimental Biology: Bethesda, MD.

Anbar,M., Guttman,S. and Lewitus,Z. (1959). The mode of action of perchlorate ions on the iodine uptake of the thyroid gland. *Int.J.Appl.Radiat.Isot.*, 7, 87-96.

Bakke, J.L., Lawrence, N.L., Robinson, S., Bennett, J. (1976). Lifelong alterations in endocrine function resulting from brief perinatal hypothyroidism in the rat. *J.Lab.Clin.Med.*, 88 (1), p.3-13.

Beaton, G.H., Beare, H., Ryu, M.H. and McHenry, E.W. (1954). Protein metabolism in the pregnant rat. *J.Nutr.*, 54, p. 291-304.

Brown, R.P., Delp, M.D., Lindstedt, S.L., Rhomberg, L.R., and Beliles, R.P. (1997). Physiological parameter values for physiologically based pharmacokinetic models. *Toxicol.Ind.Health*, 13, p. 407-484.

Brown-Grant, K. (1961). Extrathyroidal iodide concentrating mechanisms. *Physiol.Rev.*, 41, p. 189-213.

Brown-Grant, K. and Pethes, G. (1959). Concentration of radioiodine in the skin of the rat. *J.Physiol.*, 148, p. 683-693.

Buelke-Sam, J., Nelson, C.J., Byrd, R.A., and Holson, J.F. (1982a). Blood flow during pregnancy in the rat: I. Flow patterns to maternal organs. *Teratology*, 26, p. 269-277.

Buelke-Sam, J., Holson, J.F., and Nelson, C.J. (1982b). Blood flow during pregnancy in the rat: II. Dynamics of and litter variability in uterine flow. *Teratology*, 26, p. 279-288.

Carpenter, E. (1959). Development of the fetal rat thyroid with special reference to the uptake of radioactive iodine. *J.Exper.Zool.*, 142, p. 247-257.

Carr, C.W. (1952). Studies on the binding of small ions in protein solutions with the use of membrane electrodes. I. The binding of the chloride ion and other inorganic anions in solutions of serum albumin. *Arch.Biochem.Biophys.*, 40, p.286-294.

Chow, S.Y., Chang, L.R. and Yen, M.S. (1969). A comparison between the uptakes of radioactive perchlorate and iodide by rat and guinea pig thyroid glands. *J.Endocrinol.*, 45(1), p. 1-8.

Chow, S.Y. and Woodbury, D.M. (1970). Kinetics of distribution of radioactive perchlorate in rat and guinea-pig thyroid glands. *J.Endocrinol.*, 47(2), p. 207-218.

Clewell, R.A., Merrill, E.M., Yu, K.O., Mahle, D.A., Sterner, T.R., Robinson, P.J., and Gearhart, J.M. (2001). Physiologically-Based Pharmacokinetic Model for the Kinetics of Perchlorate-Induced Inhibition of Iodide in the Lactating and Neonatal Rat. AFRL-HE-WP-CL-0006.

Conde, E., Martin-Lacave, I., Godalez-Campora, R., Galera-Davidson, H. (1991) Histometry of normal thyroid glands in neonatal and adult rats. *Am.J.Anat.*, 191, p. 384-390.

Clos, J., Crepel, F., Legrand, C., Legrand, J., Rabie, A., Vigouroux, E. (1974). Thyroid physiology during the postnatal period in the rat: A study of the development of thyroid function and of the morphogenetic effects of thyroxine with special reference to cerebellar maturation. *Gen.Comp.Endocrinol.*, 23, p. 178-192.

Delange, F. (2000). The role of iodine in brain development. *Proc.Nutr.Soc.*, 59, p. 75-79.

Dobbing, J., (1974), in *Scientific Foundations of Paediatrics*, ed. Daris, J., Dobbing, J., Heineman, J. London, p. 565.

Eguchi, Y., Fukiishi, Y., Hasegawa, Y. (1980). Ontogeny of the pituitary-thyroid system in fetal rats: observations on the fetal thyroid after maternal treatment with goitrogen. *Anat.Rec.*, 198, 4, p. 637-642.

Feldman, J.D., Vazquez, J.J., and Kurtz, S.M. (1961). Maturation of the Fetal Thyroid. *J.Biophys.Biochem.Cytol.*, 11, p. 365-383.

Fisher, J.W., Whittaker, T.A., Taylor, D.H., Clewell, H.J., and Andersen, M.E. (1989). Physiologically based pharmacokinetic modeling of the pregnant rat: a multiroute exposure model for trichloroethylene and its metabolite, trichloroacetic acid: *Toxicol.Appl.Pharmacol.*, 99, p. 395-414.

Florsheim, W.H., Faircloth, M.A., Corcorran, N.L., and Rudko. (1966). Perinatal Thyroid Function in the Rat. *Acta Endocrinol.*, 32, p. 375-332.

Geloso, J.P., (1961). Date de l'entrée en fonction de la thyroïde chez le fœtus de rat. *C.R.Soc.Biol. (Paris)*, 155, p. 1239-1244.

Gluzman, B.E. and Niepomniszcze, H. (1983). Kinetics of the iodide trapping mechanism in normal and pathological human thyroid slices. *Acta Endocrinol.*, 103, p. 34-39.

Goedbloed, J.F. (1972). The embryonic and postnatal growth of rat and mouse. I. The embryonic and early postnatal growth of the whole embryo. A model with exponential growth and sudden changes in growth rate. *Acta Anat.Basel.*, 82, p. 305-306.

Gokmen I.G. and Dag, G. (1995), Determination of Iodine Content in human Milk, Cow's Milk and Infant Formula and Estimation of Daily Iodine Intake of Infants. *Analyst*, 120, p. 2005-2008.

Golstein, P., Abramow, M., Dumont, J.E., and Beauwens, R. (1992). The iodide channel of the thyroid: a membrane vesicle study. *Am.J.Physiol.*, 263 (3 pt.1), p. C590-597.

Haddow, J.E., Palomaki, G.E., Allan, W.C., Williams, J.R., Knight, G.J., Gagnon, J., O'Heir, C.E., Mitchell, M.L., Hermos, R.J., Waisbren, S.E., Faix, J.D., Klein, R.Z. (1999). Maternal

Thyroid Deficiency During Pregnancy and Subsequent Neuropsychological Development of the Child. *New Eng.J.Med.*, 341, (8), p. 549-555.

Halmi,N.S. and Stuelke,R.G. (1959). Comparison of Thyroidal and Gastric Iodide Pumps in Rats. *Endocrinology*, 64, p.103-109.

Halmi,N.S., Stuelke,R.G. and Schnell,M.D. (1956 ). Radioiodide in the thyroid and in other organs of rats treated with large doses of perchlorate. *Endocrinology*, 58, p. 634-650.

Hanwell, A., and Linzell, J.L. (1973) The time course of cardiovascular changes in the rat. *J.Physiol.*, 233, p. 99-109.

Harden,R.G., Alexander,W.D., Shimmins,J., and Robertson,J.W. (1968). A comparison between the inhibitory effect of perchlorate on iodide and pertechnetate concentrations in saliva in man. *Q.J.Exp.Physiol.Cogn.Med.Sci.*, 3 (53), p.227-238.

Hays M.T. and Green, F.A. (1973). In vitro studies of  $^{99m}\text{Tc}$ -Pertechnetate binding by human serum and tissues. *J.Nucl.Med.*, 14 (3), p.149-158.

Hetzel, B.S. and Dunn, J.T., (1989) *Ann.Rev.Nutr.*, 9, p. 21

Honour,A.J., Honour,A.J., Rowlands,E.N. (1952). Secretion of radioiodine in digestive juices and milk in man. *Clin.Sci.*, 11, p. 447-463.

Klein, A.H., Meltzer, S., Kenny, F.M., (1972). Improved prognosis in congenital hypothyroidism treated before age three months. *J.Pediatr.*, 81, (5), p. 912-915.

Knight, C.H., Docherty, A.H., and Peaker, M., (1984). Milk yield in the rat in relation to activity and size of the mammary secretory cell population. *J.Dairy.Res.*, 51, p. 29-35.

Knight, C.H and Peaker, M. (1982). Mammary cell proliferation in mice during pregnancy and lactation in relation to milk yield. *Q.J.Exp.Phys.*, 67, p. 165-177.

Kohn MC, Sewall CH, Lucier GW, Portier CJ. (1996). A mechanistic model of effects of dioxin on thyroid hormones in the rat. *Toxicol.Appl.Pharmacol.* 136(1):29-48.

Kotani,T., Ogata,Y., Yamamoto,I., Aratake,Y., Kawano,J.I., Suganuma,T., Ohtaki,S. (1998). Characterization of gastric  $\text{Na}^+/\text{I}^-$  symporter of the rat. *Clin.Immunol.Immunopathol.*, 89 (3), p. 271-278.

Kotyk, A. and K. Janacek. 1977. *Membrane Transport. An Interdisciplinary Approach.* Plenum Press, NY.

Lazarus, J.H., Harden, R.M., and Robertson, J.W.K. (1974). Quantitative studies of the inhibitory effect of perchlorate on the concentration of  $^{36}\text{ClO}_4^-$ ,  $^{125}\text{I}^-$ , and  $^{99m}\text{TcO}_4^-$  in salivary glands of male and female mice. *Arch.Oral.Biol.*, 19, p.493-498.

Malendowicz, L.K., and Bednarek, J. (1986). Sex dimorphism in the thyroid gland. *Acta Anat.*, 127, p. 115-118.

Mattie, D.R., Jarabek, AM. (1999). Perchlorate Environmental Contamination: Testing Strategy Based on Mode of Action. *The Toxicologist. Toxicol.Sci.*, 48, 113.

Merrill EA, Clewell RA, Gearhart JM, Robinson PT, Sterner TR, Yu KO, Narayanan L, and Fisher JW. 2001a. PBPK Model for Perchlorate-Induced Inhibition in the Male Rat. AFRL-HE-WP-CL-0005.

Merrill EA, Clewell RA, Sterner TR, Gearhart JM. 2001b. PBPK Model for Perchlorate-Induced Inhibition of Radioiodide Uptake in Humans AFRL-HE-WP-CL-0008.

Myant, N.B. (1971). The role of thyroid hormone in the fetal and postnatal development of mammals. in *Hormones in Development*. Appleton-Century-Crofts, NY., p. 465-471.

Naismith, D.J., Richardson, D.P., and Pritchard, A.E. (1982). The utilization of protein and energy during lactation in the rat, with particular regard to the use of fat accumulated during pregnancy. *Br.J.Nutr.*, 48, p.433-441.

Nataf, B. and Sfez, M. (1961). Debut du fonctionnement de la thyroide foetale du rat. *C.R.Soc.Biol. (Paris)*, 55, p.1235-1238.

Perlman,I., Chaikoff,I.L. and Morton,M.E. (1941). Radioactive iodine as an indicator of the metabolism of iodine. I. The turnover of iodine in the tissues of the normal animal, with particular reference to the thyroid. *J.Biol.Chem.*, 149, p. 433-447.

Pena,H.G.; Kessler,W.V.; Christian,J.E.; Cline,T.R.; Plumlee,M.P. (1976). A comparative study of iodine and potassium perchlorate metabolism in the laying hen. 2. Uptake, distribution, and excretion of potassium perchlorate. *Poult.Sci.*, 55(1), p. 188-201.

Porterfield, S.P. (1994). Vulnerability of the Developing Brain to Thyroid Abnormalities: Environmental Insults to the Thyroid System. *Environ.Health Perspect.*, 102 (Suppl 2), p. 125-130.

O'Flaherty, E.J., Scott, W., Schreiner, C., Beliles, R. P. (1992). A physiologically based kinetic model of rat and mouse gestation: disposition of a weak acid. *Toxicol.Appl.Pharmacol.*, 112, p. 245-256.

Roti, E., Gnudi, A., Braverman, L.E. (1983). The Placental Transport, Synthesis and Matabolism of Hormones and Drugs which Affect Thyroid Function. *Endocrine Rev.*, 4, p. 131-149.

Scatchard, G. and Black, E.S. (1949). The effects of salts on the isoionic and isoelectric points of proteins. *J.Phys.Colloid Chem.*, 53, p. 88-99.

Shishiba, Y., Shimizu, T., Yoshimura, S. and Shimizu, K. (1970). [Effect of thiocyanate and perchlorate on free thyroxine fraction]. *Nippon.Naibunpi.Gakkai.Zasshi.*, 46 (1), p. 16-19.

Sikov, M.R. and Thomas, J.M. (1970) Prenatal growth of the rat. *Growth*, 34, p. 1-14.

Spitzweg, C., Joba, W., Eisenmenger, W. and Heufelder, A.E. (1998). Analysis of human sodium iodide symporter gene expression in extrathyroidal tissues and cloning of its complementary deoxyribonucleic acids from salivary gland, mammary gland, and gastric mucosa. *J.Clin.Endocrinol.Metab.*, 83, p. 1746-1751.

Sztanyik, L.B. and Turai, I. (1988). Modification of Radioiodine Incorporation in the Fetus and Newborn Rats by the Thyroid Blocking Agents. *Acta Phys.Hungaria.*, 72, p.343-354.

Tazebay, U.H., Wapnir, I.L., Levy, O., Dohan, O., Zuckier, L.S., Zhao, Q.H., Deng, H.F., Amenta, P.S., Fineberg, S., Pestell, R.G., Carrasco, N. (2000). The mammary gland iodide transporter is expressed during lactation and in breast cancer. *Nat.Med.*, 6(8), p.871-878.

Urbansky, E.T. (1998). Perchlorate chemistry: implications for analysis and remediation. *Bioremed.J.*, 2(2), p. 81-95.

Urbansky, E.T., and Schock, M.R. (1999). Issue in managing risks associated with perchlorate in drinking water. *J.Environ.Management*, 56, p. 79-95.

Versloot, P.M., Schroder-Van Der Elst, J.P., Van Der Heide, D., and Boogerd, L. (1997). Effects of marginal iodine deficiency during pregnancy: iodide uptake by the maternal and fetal thyroid. *Am.J.Physiol.*, 273 (6 pt. 1), E1121-E1126.

Wolff, J. (1998) Perchlorate and the Thyroid Gland. *Pharmacolog.Rev.*, 50, p. 89-105.

Wolff, J. and Maurey, J.R. (1961) Thyroidal iodide transport: II. Comparison with non-thyroid iodide-concentrating tissues. *Biochim.Biophys.Acta*, 47, p. 467-474.

Wolff, J. and Maurey, J.R. (1963) Thyroidal Iodide Transport: IV. The Role of Ion Size. *Biochim.Biophys.Acta*, 69, p. 48-58.

Yamada, T. (1967). Effects of perchlorate and other anions on thyroxin metabolism in the rat. *Endocrinology*, 81, p. 1285-1290.

Yu, K.O, Mahle, D.A., Narayanan, L., Godfrey, R.J., Butler, G.W., Todd, P.N., Parish, M.A., McCafferty, J.D., Ligman, T.A., Goodyear, C.D., Sterner, T.R., Bausman, T.A., Mattie, D.R., Fisher, J.W. (2000a). Tissue Distribution and Inhibition of Iodide Uptake in the Thyroid by Perchlorate with Corresponding Hormonal Changes in Pregnant and Lactating Rats (drinking water study). AFRL-HE-WP-CL-0038.

Yu, K.O., Narayanan, L., Godfrey, R.J., Todd, P.N., Goodyear, C.D., Sterner, T.R., Bausman, T.A., Young, S.M., Mattie, D.R., Fisher, J.W. (2000b). Effects of Perchlorate on Thyroidal Uptake of Iodide with Corresponding Hormonal Changes. AFRL-HE-WP-TR-2000-0076.

Zeghal, N., Redjem, M., Gondran, F. and Vigouroux, E. (1995). [Analysis of iodine compounds in young rat skin in the period of suckling and in the adult. Effect of perchlorate]. Arch. Physiol. Biochem., 103 (4), p. 502-511.

## **GD20 Inhibition Statistical Summary**

**Charles D. Goodyear**

Free and bound iodide in the maternal serum, fetal serum (pooled across pups), and maternal thyroid were determined for 6 dams in each of 14 groups. The 14 groups consisted of a control group and a 1 mg/kg group at each of 7 time-points (0.5, 1, 2, 4, 8, 12, and 24 hours). For each time-point, the Wilcoxon Rank Sum test (2-tailed) was performed to determine whether the control and 1 mg/kg dose groups were significantly different. A non-parametric test was used since there were instances of non-normal distributions among the 6 dams. In some groups, there were 1 or 2 dams that had values substantially different from the other dams in the same group. In addition to comparing free and bound iodide, total iodide (sum of bound and free) was also compared.

Figures 1, 2, and 3 contain the values for each dam along with a line segment connecting means from each group. The legend on the figures is the rank order of the rat # for each combination of dose group and time-point. Tables 1, 2, and 3 contain means and standard deviations of dams (or litters for iodide in fetal serum) along with p-values from the Wilcoxon Rank Sum test.

For the 1 mg/kg dose group at time-point = 4 hours, there were only 5 dams.



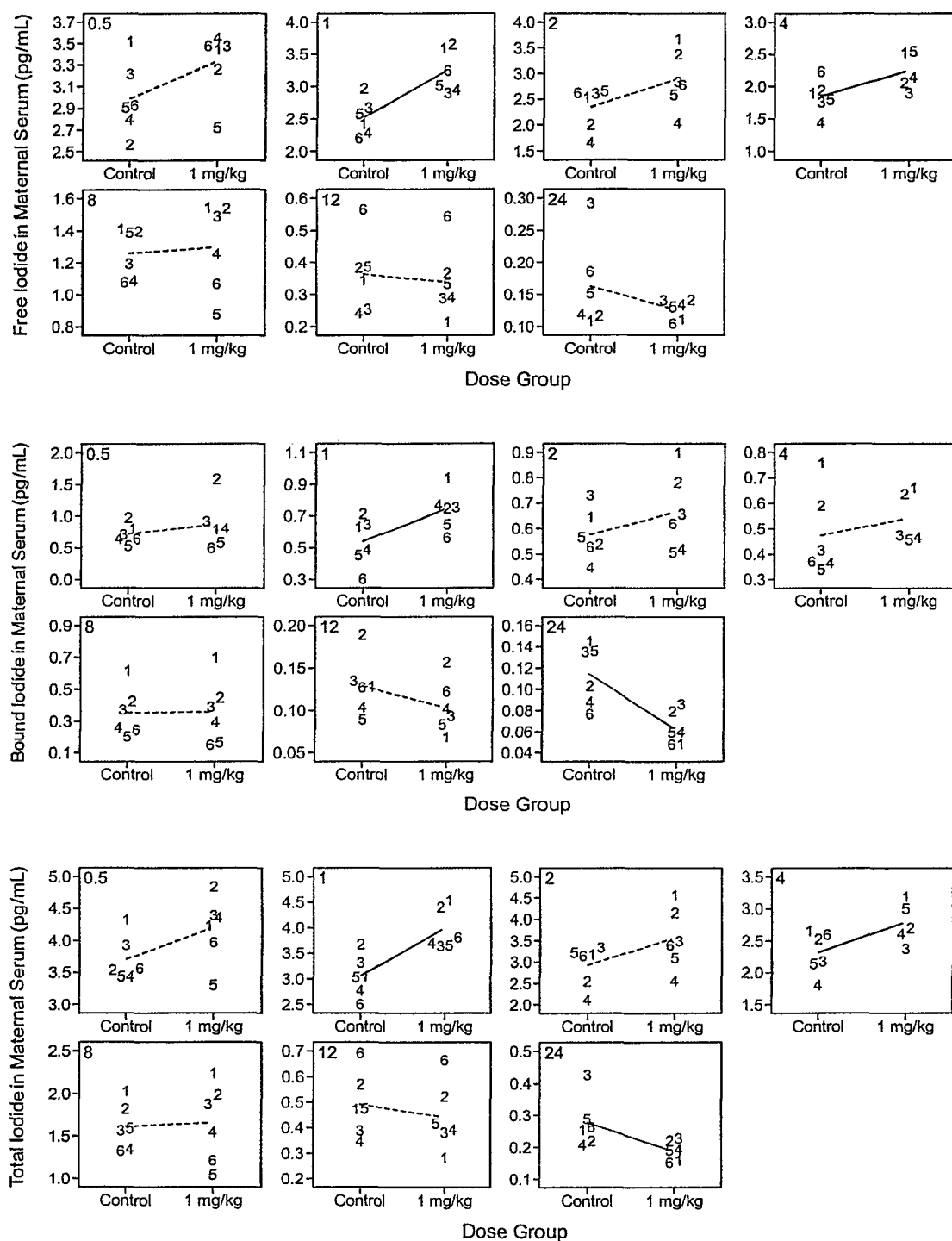


Figure 1. Iodide in Maternal Serum for each Dam. Time-points (hours) are located in the upper left corner of each plot. Line segments connect means from the dose groups. A solid line indicates a significant difference ( $p \leq 0.05$ ) while a dashed line indicates no significant difference. The legend is the rank order of the rat # in each combination of dose group and time-point.

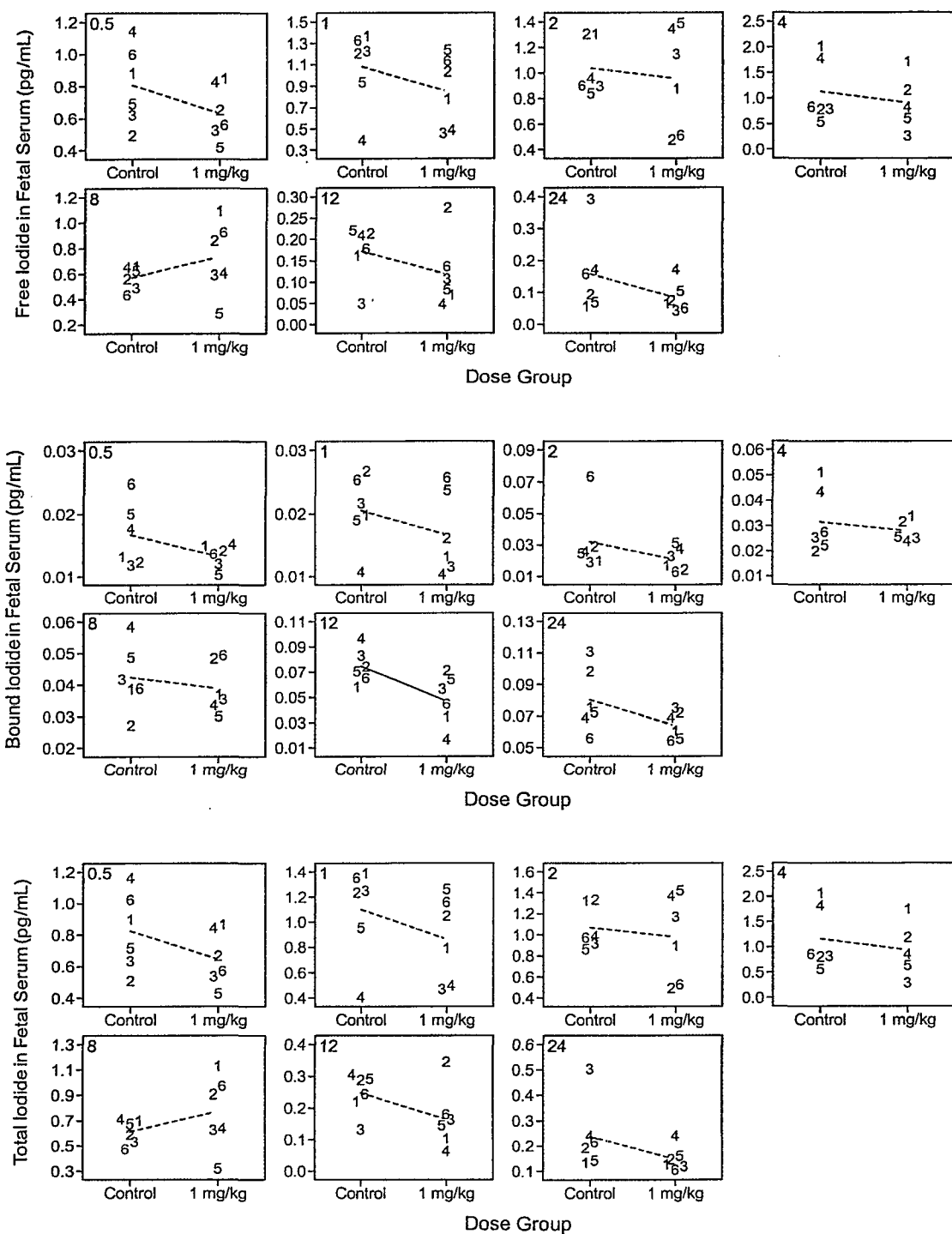


Figure 2. Iodide in Fetal Serum for each Litter. Time-points (hours) are located in the upper left corner of each plot. Line segments connect means from the dose groups. A solid line indicates a significant difference ( $p \leq 0.05$ ) while a dashed line indicates no significant difference. The legend is the rank order of the rat # in each combination of dose group and time-point.

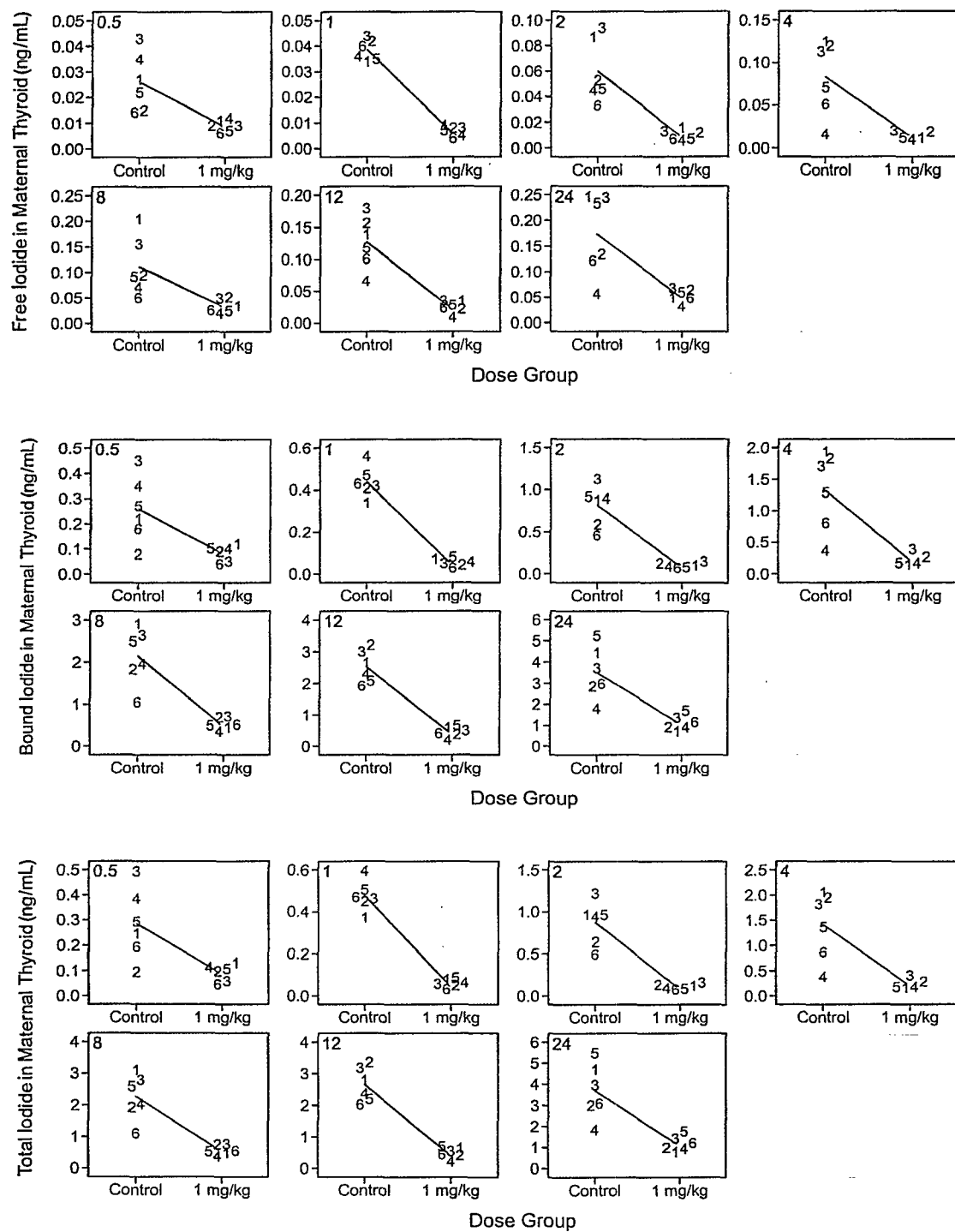


Figure 3. Iodide in Maternal Thyroid for each Dam. Time-points (hours) are located in the upper left corner of each plot. Line segments connect means from the dose groups. A solid line indicates a significant difference ( $p \leq 0.05$ ) while a dashed line indicates no significant difference. The legend is the rank order of the rat # in each combination of dose group and time-point.

Time (hours)	Type	Control			1 mg/kg			Percent Change	P-value
		N	Mean	Std	N	Mean	Std		
0.5	Free	6	2.989	0.334	6	3.323	0.310	11	0.1495
	Bound	6	0.718	0.155	6	0.862	0.385	20	0.6310
	Total	6	3.706	0.353	6	4.186	0.517	13	0.1093
1	Free	6	2.520	0.281	6	3.224	0.335	28	0.0104
	Bound	6	0.539	0.153	6	0.736	0.128	37	0.0250
	Total	6	3.059	0.412	6	3.960	0.401	29	0.0104
2	Free	6	2.349	0.413	6	2.878	0.580	23	0.0782
	Bound	6	0.575	0.100	6	0.664	0.153	15	0.4233
	Total	6	2.924	0.486	6	3.542	0.726	21	0.1093
4	Free	6	1.842	0.258	5	2.234	0.288	21	0.0446
	Bound	6	0.473	0.167	5	0.539	0.102	14	0.2012
	Total	6	2.315	0.334	5	2.773	0.322	20	0.0446
8	Free	6	1.259	0.158	6	1.296	0.277	3	0.6310
	Bound	6	0.353	0.154	6	0.359	0.206	2	1.0000
	Total	6	1.613	0.274	6	1.655	0.466	3	1.0000
12	Free	6	0.362	0.117	6	0.339	0.112	-6	0.5218
	Bound	6	0.129	0.034	6	0.104	0.031	-19	0.1495
	Total	6	0.491	0.126	6	0.444	0.133	-10	0.5218
24	Free	6	0.162	0.069	6	0.127	0.015	-22	0.4233
	Bound	6	0.114	0.029	6	0.064	0.016	-44	0.0104
	Total	6	0.277	0.079	6	0.191	0.030	-31	0.0250

Table 1. Test results for Iodide in Maternal Serum (pg/mL). P-values are from the Wilcoxon Rank Sum test (2-tailed).

Time (hours)	Type	Control			1 mg/kg			Percent Change	P-value
		N	Mean	Std	N	Mean	Std		
0.5	Free	6	0.806	0.244	6	0.639	0.172	-21	0.2002
	Bound	6	0.017	0.005	6	0.013	0.002	-20	0.4233
	Total	6	0.823	0.247	6	0.652	0.174	-21	0.2002
1	Free	6	1.077	0.367	6	0.855	0.332	-21	0.2623
	Bound	6	0.021	0.006	6	0.017	0.006	-18	0.3367
	Total	6	1.098	0.372	6	0.872	0.338	-21	0.2623
2	Free	6	1.035	0.213	6	0.959	0.400	-7	0.8728
	Bound	6	0.032	0.021	6	0.021	0.008	-35	0.2623
	Total	6	1.067	0.209	6	0.980	0.408	-8	0.8728
4	Free	6	1.132	0.612	5	0.922	0.555	-19	0.7150
	Bound	6	0.032	0.013	5	0.028	0.005	-11	1.0000
	Total	6	1.163	0.625	5	0.950	0.559	-18	0.5839
8	Free	6	0.570	0.093	6	0.727	0.288	28	0.3367
	Bound	6	0.042	0.011	6	0.039	0.008	-8	0.4233
	Total	6	0.612	0.097	6	0.766	0.293	25	0.3367
12	Free	6	0.172	0.064	6	0.119	0.082	-31	0.2002
	Bound	6	0.075	0.014	6	0.048	0.020	-36	0.0250
	Total	6	0.247	0.065	6	0.167	0.097	-32	0.1495
24	Free	6	0.158	0.124	6	0.085	0.048	-46	0.2290
	Bound	6	0.080	0.020	6	0.064	0.009	-20	0.0921
	Total	6	0.238	0.136	6	0.150	0.049	-37	0.1275

Table 2. Test results for Iodide in Fetal Serum (pg/mL). P-values are from the Wilcoxon Rank Sum test (2-tailed).

Time (hours)	Type	Control			1 mg/kg			Percent Change	P-value
		N	Mean	Std	N	Mean	Std		
0.5	Free	6	0.026	0.011	6	0.009	0.002	-65	0.0039
	Bound	6	0.258	0.130	6	0.083	0.031	-68	0.0247
	Total	6	0.284	0.141	6	0.092	0.033	-68	0.0250
1	Free	6	0.039	0.004	6	0.007	0.002	-82	0.0039
	Bound	6	0.438	0.073	6	0.056	0.019	-87	0.0039
	Total	6	0.477	0.073	6	0.063	0.020	-87	0.0039
2	Free	6	0.060	0.025	6	0.010	0.004	-83	0.0039
	Bound	6	0.813	0.244	6	0.103	0.029	-87	0.0039
	Total	6	0.873	0.262	6	0.113	0.032	-87	0.0039
4	Free	6	0.083	0.044	5	0.015	0.005	-82	0.0174
	Bound	6	1.325	0.626	5	0.230	0.101	-83	0.0104
	Total	6	1.408	0.670	5	0.245	0.105	-83	0.0106
8	Free	6	0.111	0.058	6	0.034	0.014	-70	0.0065
	Bound	6	2.148	0.675	6	0.543	0.141	-75	0.0039
	Total	6	2.260	0.725	6	0.577	0.153	-74	0.0039
12	Free	6	0.127	0.041	6	0.026	0.010	-80	0.0039
	Bound	6	2.525	0.517	6	0.468	0.163	-81	0.0039
	Total	6	2.652	0.548	6	0.494	0.171	-81	0.0039
24	Free	6	0.173	0.080	6	0.054	0.013	-69	0.0163
	Bound	6	3.513	1.232	6	1.137	0.353	-68	0.0039
	Total	6	3.687	1.304	6	1.190	0.359	-68	0.0039

Table 3. Test results for Iodide in Maternal Thyroid (ng/mL). P-values are from the Wilcoxon Rank Sum test (2-tailed).

**Serum Hormone (TSH, T<sub>3</sub>, T<sub>4</sub>) Statistical Report  
(Gestation Day 20)**

**Charles D. Goodyear**

Serum thyroid hormone levels were determined from 8 dams and 4 fetuses in each of 5 dose groups (control, 0.01, 0.1, 1, and 10 mg/kg/day). Since all 40 dams could not be handled at the same time, 10 dams were brought in at 4 different times. Two dams from each time group were assigned to each of the 5 dose groups. One fetus from each time group and dose group was used.

T<sub>3</sub>, T<sub>4</sub>, Free T<sub>4</sub>, and TSH were used as dependent variables in a one-factor (dose group) analysis of variance, performed separately for the dams and fetuses. In preliminary analyses, time group was included as a factor (for dams only). Since there were no significant main effects of time group or interactions between time group and dose group ( $0.1414 < p$ ), time group was removed as a factor. Results of the one-factor analyses are shown in table 1. Paired comparisons among the dose groups used 2-tailed t-tests with pooled error. Results are shown in tables 2-5. Note that there was an occasional missing data value.

Figures 1a, 2a, 3a, and 4a show the hormone levels for each rat and fetus along with the mean for each dose group. Figures 1b, 2b, 3b, and 4b show the mean % change from control for each dose group. Figures 5a and 5b show all hormones in the same figure.

Hormone	Rat	Source	SS	DF	SSE	DFE	F	P
T <sub>3</sub>	Dam	Dose	7.97E+02	4	2.45E+03	34	2.76	0.0433
T <sub>3</sub>	Fetus	Dose	5.75E+00	4	1.66E+01	15	1.30	0.3149
T <sub>4</sub>	Dam	Dose	7.55E+00	4	1.49E+00	34	43.07	0.0001
T <sub>4</sub>	Fetus	Dose	6.19E-02	4	6.32E-02	15	3.67	0.0282
Free T <sub>4</sub>	Dam	Dose	4.73E-01	4	6.11E-02	33	63.86	0.0001
Free T <sub>4</sub>	Fetus	Dose	1.38E-03	4	2.50E-04	15	20.63	0.0001
TSH	Dam	Dose	1.50E+02	4	1.92E+01	34	66.36	0.0001
TSH	Fetus	Dose	2.75E+01	4	6.40E+00	15	16.09	0.0001

Table 1. Analysis of variance results. The dependent variable was hormone level.

Rat	Dose Group mg/kg/day	N	Mean T <sub>3</sub> (ng/dL)	Std Dev T <sub>3</sub> (ng/dL)	Dose Group mg/kg/day			
					0.01	0.1	1	10
Dam	Control	8	102.9	6.1	0.5291	0.1649	0.0372	0.0059
	0.01	8	100.2	8.3		0.4388	0.1293	0.0277
	0.1	8	96.9	8.4			0.4305	0.1387
	1	7	93.4	9.7				0.5092
	10	8	90.5	9.6				
Fetus	Control	4	15.0	0.7	0.5098	0.4575	0.1191	0.0633
	0.01	4	14.5	1.4		0.9316	0.3438	0.2033
	0.1	4	14.4	0.6			0.3874	0.2329
	1	4	13.7	1.2				0.7292
	10	4	13.5	1.1				

Table 2. Paired comparisons of dose group for T<sub>3</sub>. Values listed under each dose column are p-values (2-tailed t-test with pooled error) for comparing row dose and column dose.

Rat	Dose Group mg/kg/day	N	Mean T <sub>4</sub> (ug/dL)	Std Dev T <sub>4</sub> (ug/dL)	Dose Group mg/kg/day			
					0.01	0.1	1	10
Dam	Control	8	2.72	0.31	0.0001	0.0001	0.0001	0.0001
	0.01	8	1.85	0.18		0.4429	0.0815	0.0006
	0.1	8	1.77	0.18			0.3034	0.0049
	1	7	1.65	0.17				0.0712
	10	8	1.45	0.16				
Fetus	Control	4	0.80	0.08	0.7809	0.1868	0.0185	0.0087
	0.01	4	0.79	0.06		0.2886	0.0324	0.0154
	0.1	4	0.74	0.08			0.2276	0.1231
	1	4	0.68	0.04				0.7123
	10	4	0.66	0.05				

Table 3. Paired comparisons of dose group for T<sub>4</sub>. Values listed under each dose column are p-values (2-tailed t-test with pooled error) for comparing row dose and column dose.



Rat	Dose Group mg/kg/day	N	Mean Free T <sub>4</sub> (ng/dL)	Std Dev Free T <sub>4</sub> (ng/dL)	Dose Group mg/kg/day			
					0.01	0.1	1	10
Dam	Control	8	0.281	0.030	0.5345	0.0001	0.0001	0.0001
	0.01	8	0.294	0.033		0.0001	0.0001	0.0001
	0.1	7	0.423	0.035			0.0003	0.0001
	1	7	0.515	0.051				0.1384
	10	8	0.548	0.058				
Fetus	Control	4	0.039	0.005	0.6712	0.0336	0.0240	0.0001
	0.01	4	0.040	0.004		0.0761	0.0552	0.0001
	0.1	4	0.045	0.003			0.8648	0.0001
	1	4	0.046	0.005				0.0001
	10	4	0.062	0.003				

Table 4. Paired comparisons of dose group for Free T<sub>4</sub>. Values listed under each dose column are p-values (2-tailed t-test with pooled error) for comparing row dose and column dose.

Rat	Dose Group mg/kg/day	N	Mean TSH (ng/mL)	Std Dev TSH (ng/mL)	Dose Group mg/kg/day			
					0.01	0.1	1	10
Dam	Control	8	4.97	0.48	0.0001	0.0001	0.0001	0.0001
	0.01	8	6.61	0.43		0.6313	0.0001	0.0001
	0.1	7	6.80	0.50			0.0002	0.0001
	1	8	8.41	0.89				0.0001
	10	8	10.70	1.15				
Fetus	Control	4	7.12	0.71	0.0915	0.0175	0.0003	0.0001
	0.01	4	7.95	0.34		0.4000	0.0113	0.0001
	0.1	4	8.35	0.62			0.0617	0.0003
	1	4	9.28	0.57				0.0164
	10	4	10.53	0.89				

Table 5. Paired comparisons of dose group for TSH. Values listed under each dose column are p-values (2-tailed t-test with pooled error) for comparing row dose and column dose.

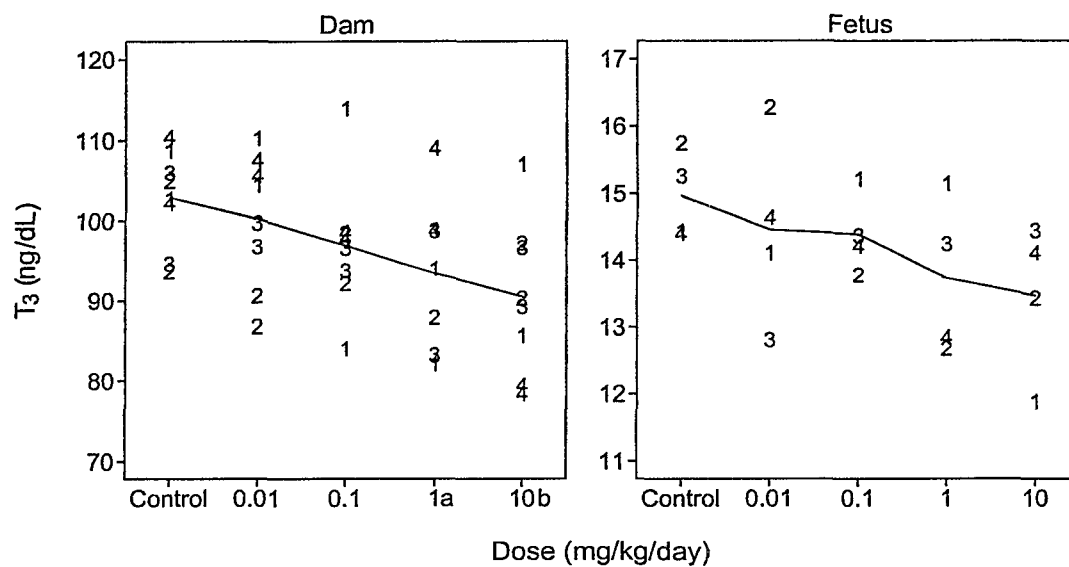


Figure 1a.  $T_3$  for each rat. Line segments connect means from each dose group. Legend is value of # for each GD20-# group. Comparisons with control (a:  $0.01 < p \leq 0.05$ , b:  $0.001 < p \leq 0.01$ , c:  $p \leq 0.001$ ) used 2-tailed t-tests with pooled error.

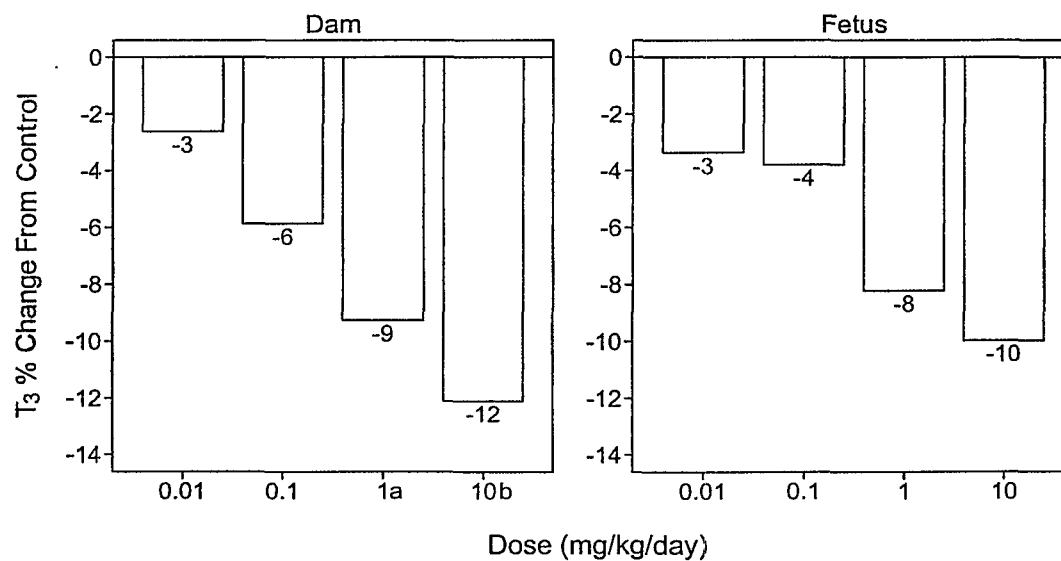


Figure 1b. Mean percent change from control for  $T_3$ . Comparisons with control (a:  $0.01 < p \leq 0.05$ , b:  $0.001 < p \leq 0.01$ , c:  $p \leq 0.001$ ) used 2-tailed t-tests with pooled error.

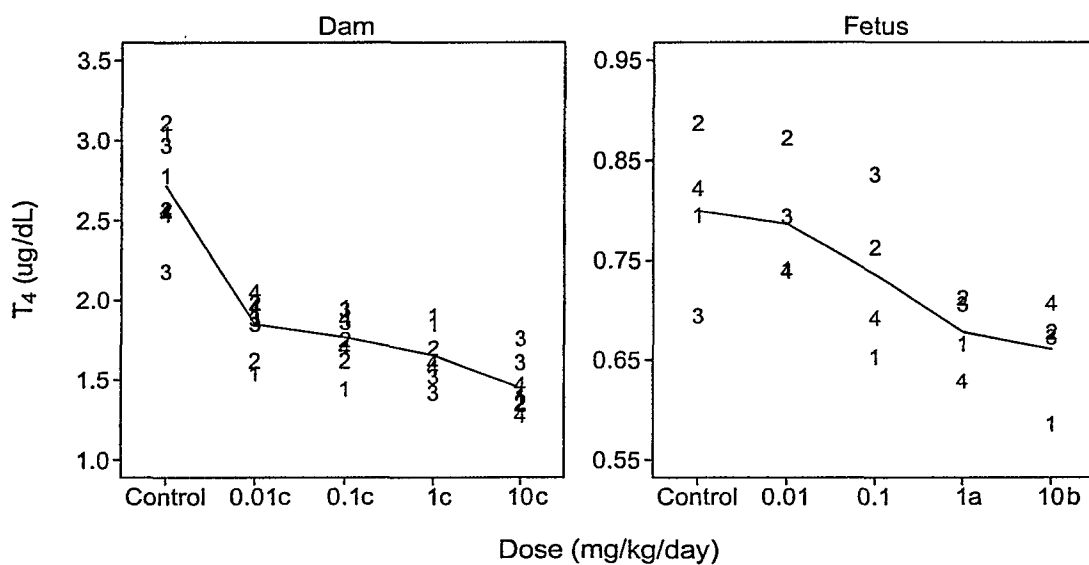


Figure 2a. T<sub>4</sub> for each rat. Line segments connect means from each dose group. Legend is value of # for each GD20-# group. Comparisons with control (a: 0.01<p≤0.05, b: 0.001<p≤0.01, c: p≤0.001) used 2-tailed t-tests with pooled error.

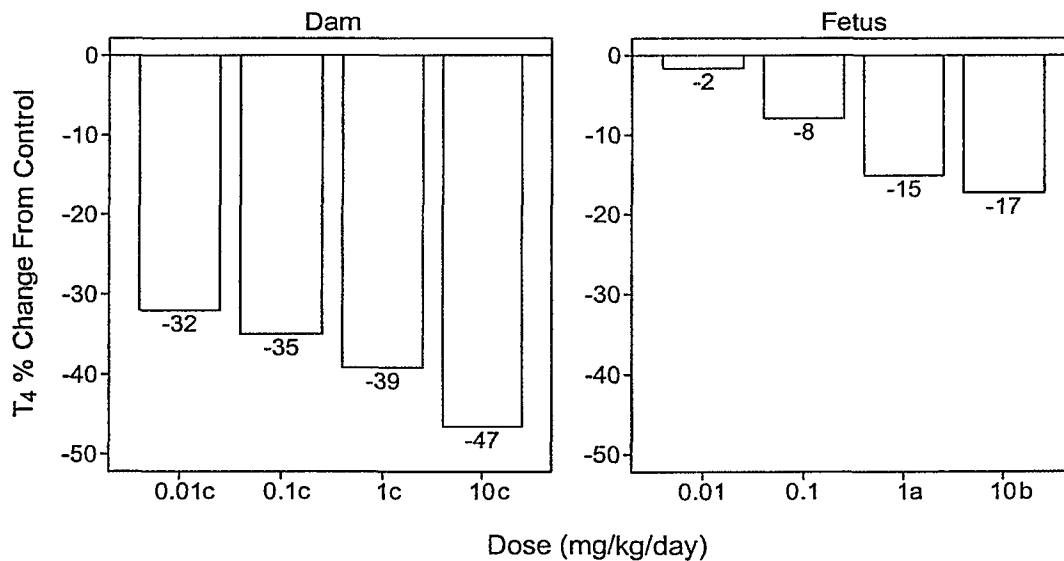


Figure 2b. Mean percent change from control for T<sub>4</sub>. Comparisons with control (a: 0.01<p≤0.05, b: 0.001<p≤0.01, c: p≤0.001) used 2-tailed t-tests with pooled error.

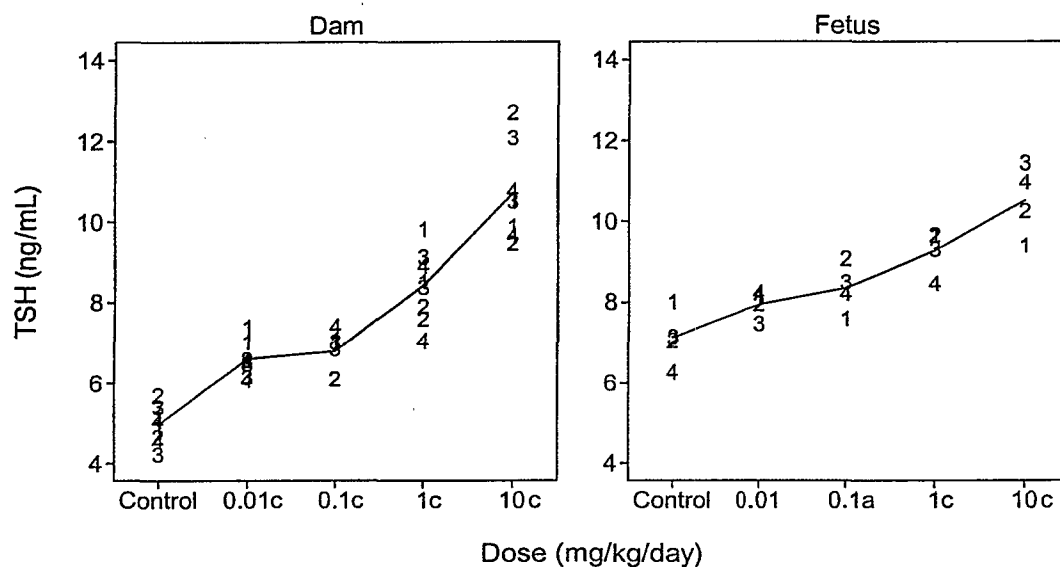


Figure 4a. TSH for each rat. Line segments connect means from each dose group. Legend is value of # for each GD20-# group. Comparisons with control (a:  $0.01 < p \leq 0.05$ , b:  $0.001 < p \leq 0.01$ , c:  $p \leq 0.001$ ) used 2-tailed t-tests with pooled error.

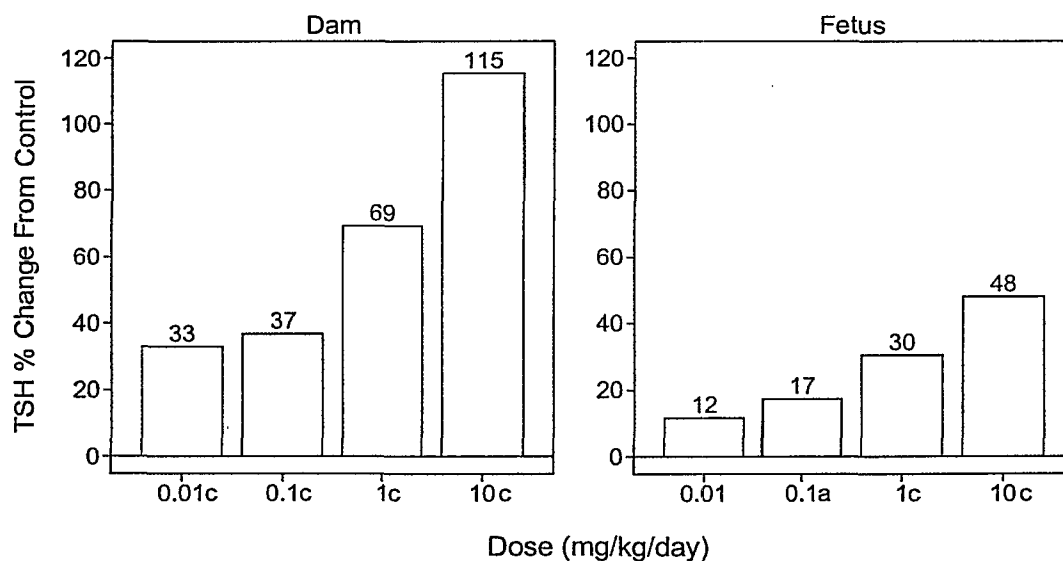


Figure 4b. Mean percent change from control for TSH. Comparisons with control (a:  $0.01 < p \leq 0.05$ , b:  $0.001 < p \leq 0.01$ , c:  $p \leq 0.001$ ) used 2-tailed t-tests with pooled error.

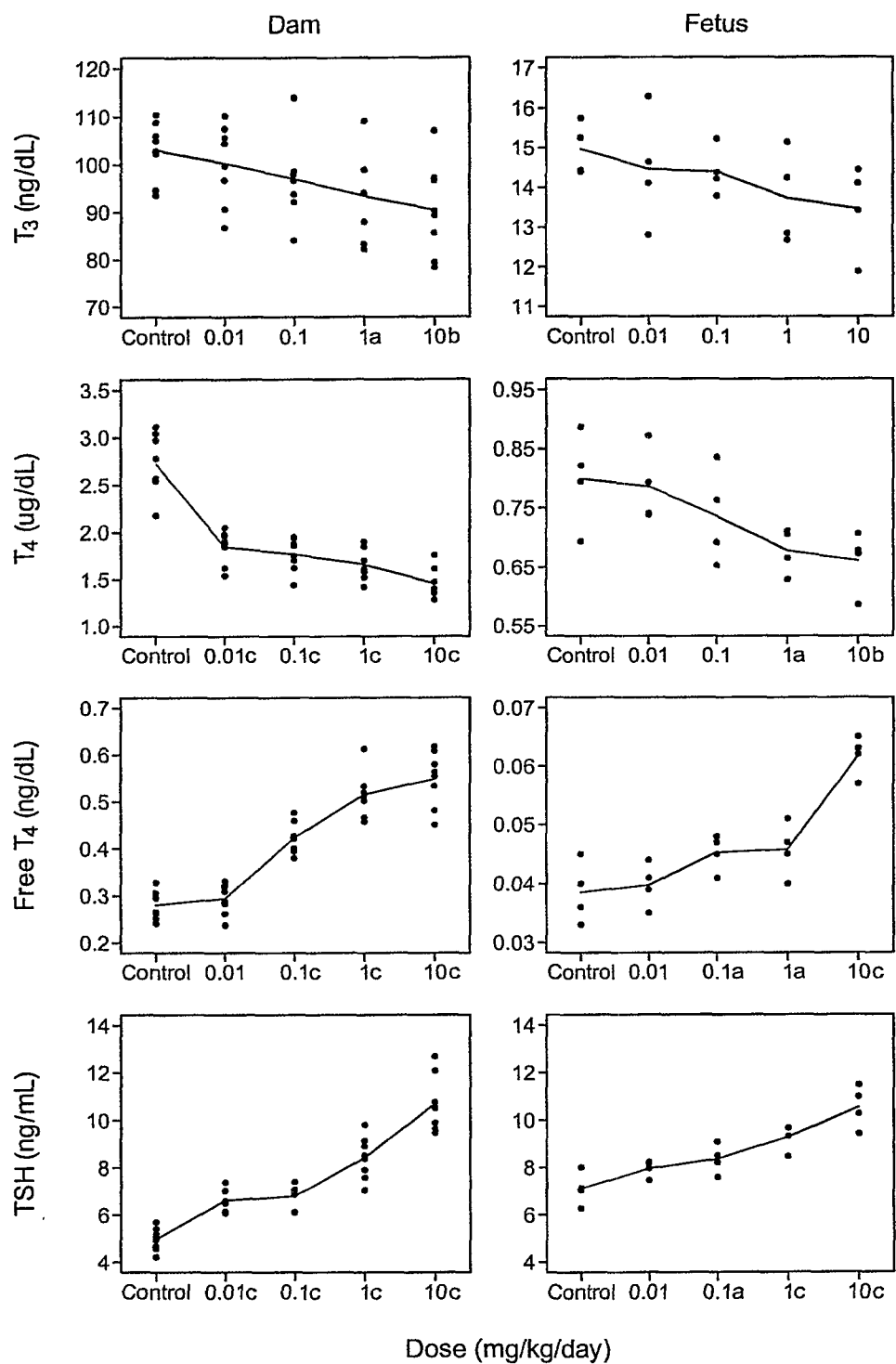


Figure 5a. Hormone level for each rat. Line segments connect means from each dose group. Comparisons with control (a:  $0.01 < p \leq 0.05$ , b:  $0.001 < p \leq 0.01$ , c:  $p \leq 0.001$ ) used 2-tailed t-tests with pooled error.

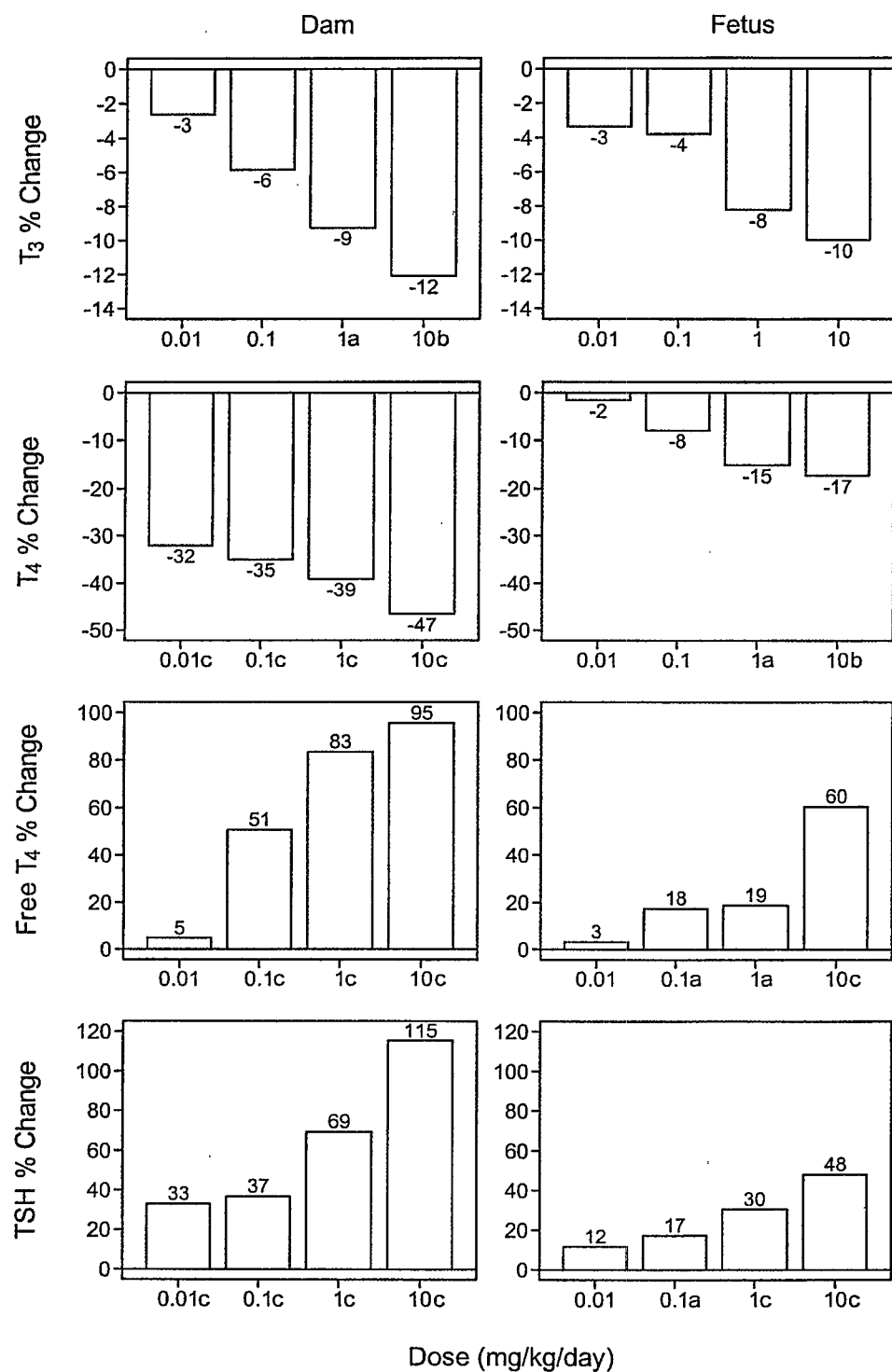


Figure 5b. Mean percent change from control. Comparisons with control (a:  $0.01 < p \leq 0.05$ , b:  $0.001 < p \leq 0.01$ , c:  $p \leq 0.001$ ) used 2-tailed tests with pooled error.